

Two-dimensional material

1

- Graphene

- symmetries
- Effective Hamiltonian

2

- Transition metal dichalcogenide

- Berry curvature
- Optical transitions

3

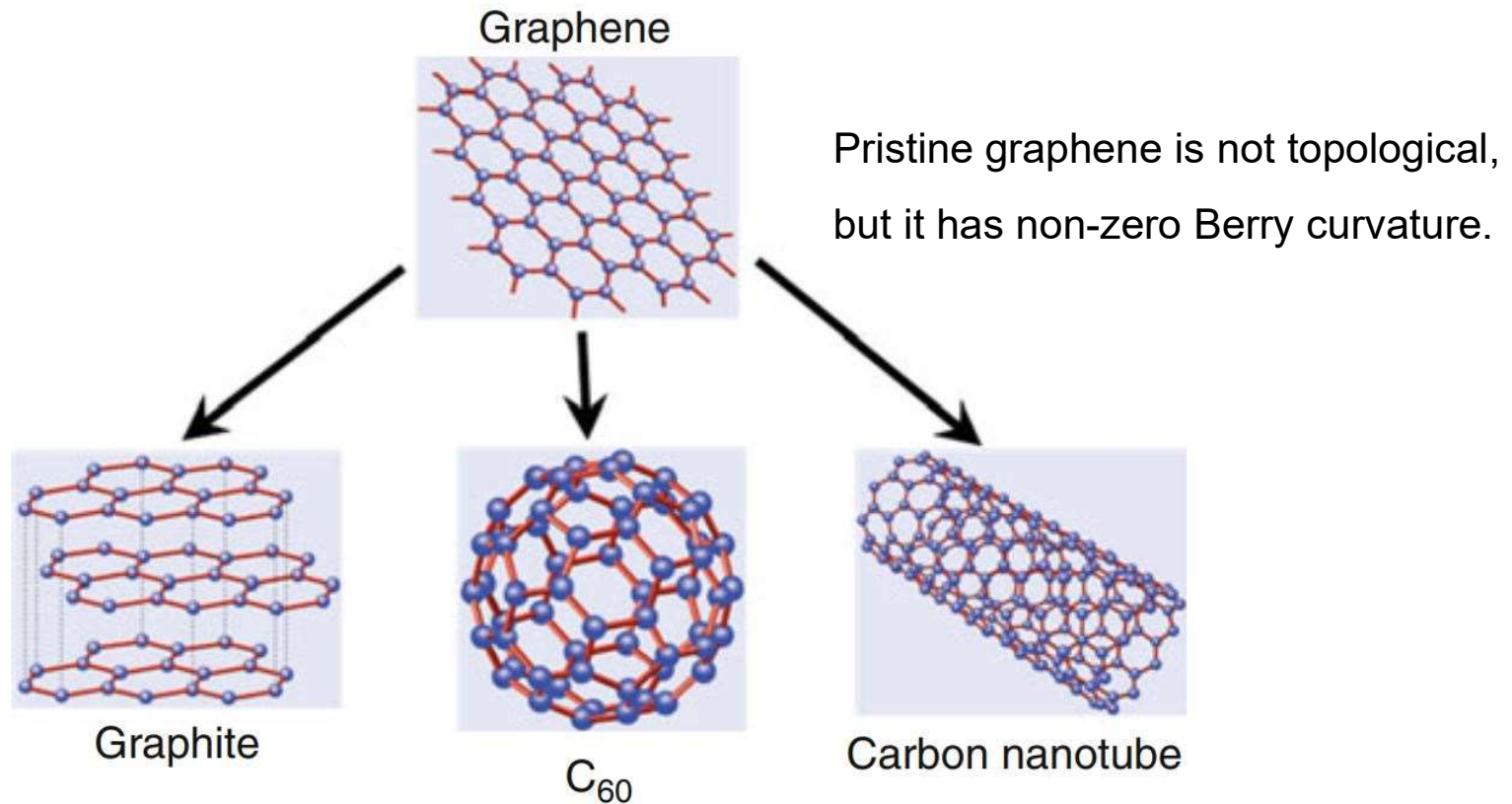
- Haldane model

- Haldane flux
- Berry curvature

4

- Twisted bilayer graphene

- 1947, [theory](#) of graphene by Wallace
- 1968, Mermin-Wagner theorem (no long-range order in 2D)
- 1985, discovery of [bucky ball](#) by Kroto, Smalley, and Curl (1996 Nobel prize)
- 1991, discovery of [carbon nanotube](#) by Iijima and Ichihashi.
- 2004, [first graphene produced](#) by Geim and Novoselov (2010 Nobel prize)



Extraordinary Properties of Graphene

- ❑ **Room-temperature electron mobility of $2.5 \times 10^5 \text{ cm}^2 \text{V}^{-1} \text{ s}^{-1}$**

Nano Lett. 11, 2396–2399 (2011).

- ❑ **Young's modulus of 1 TPa and intrinsic strength of 130 GPa, the strongest materials ever tested.**

Cu: 0.117 TPa

Phys. Rev. B 76, 064120 (2007).

- ❑ **High thermal conductivity: above $3,000 \text{ Wm}^{-1} \text{K}^{-1}$**

Cu: $401 \text{ Wm}^{-1} \text{K}^{-1}$

Nature Mater. 10, 569–581 (2011).

- ❑ **A prediction in 2015 suggested a melting point at least 5000 K.**

- ❑ **Optical absorption of 2.3%**

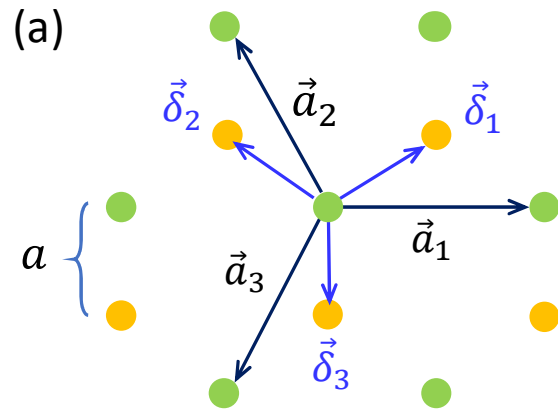
Science 320, 1308 (2008).

- ❑ **No band gap for undoped graphene**

- ❑ **The electrical resistivity of graphene $< 10^{-6} \Omega \cdot \text{cm}$, less than silver, the lowest known at RT.**

From Raynien Kwo's ppt

1 Graphene lattice



- Lattice vectors

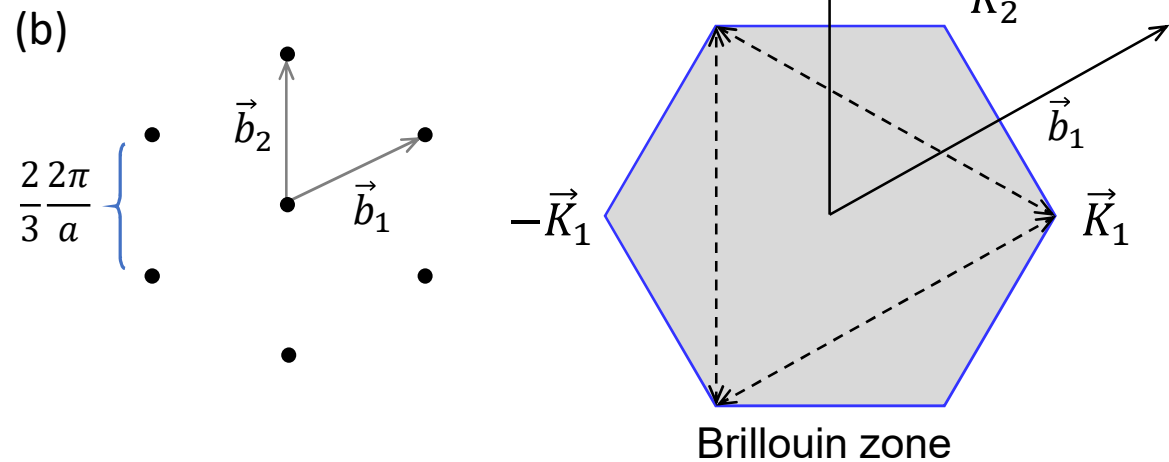
$$\mathbf{a}_1 = \sqrt{3}a\hat{x},$$

$$\mathbf{a}_2 = -\frac{\sqrt{3}}{2}a\hat{x} + \frac{3}{2}a\hat{y},$$

$$\mathbf{a}_3 = -\frac{\sqrt{3}}{2}a\hat{x} - \frac{3}{2}a\hat{y}.$$

$$a = 1.42 \text{ \AA}$$

$$a_0 = \sqrt{3}a \simeq 2.46 \text{ \AA}$$



- Reciprocal lattice vectors

$$\mathbf{b}_1 = \frac{2\pi}{a} \left(\frac{1}{\sqrt{3}}\hat{x} + \frac{1}{3}\hat{y} \right),$$

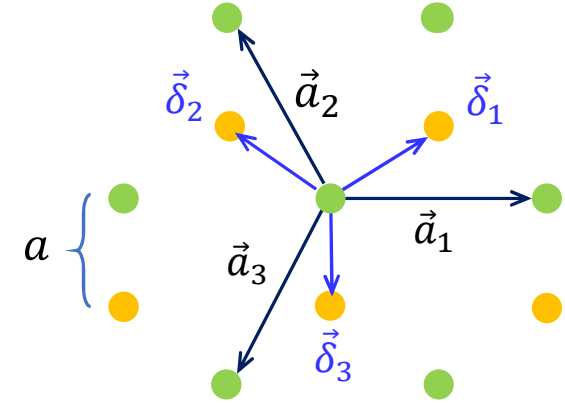
$$\mathbf{b}_2 = \frac{2\pi}{a} \frac{2}{3}\hat{y}.$$

Tight-binding model
(spin neglected)

$$\hat{H} = \hat{H}_{NN} + \hat{H}_{NNN} + \hat{H}_{on-site}.$$

$$(1) \quad \hat{H}_{NN} = t_1 \sum_{\mathbf{R}} \left(d_{\mathbf{R}+\delta_1}^\dagger c_{\mathbf{R}} + d_{\mathbf{R}+\delta_2}^\dagger c_{\mathbf{R}} + d_{\mathbf{R}+\delta_3}^\dagger c_{\mathbf{R}} \right) + h.c.$$

$$\begin{aligned} \delta_1 &= \frac{\sqrt{3}}{2} a \hat{x} + \frac{1}{2} a \hat{y}, \\ \delta_2 &= -\frac{\sqrt{3}}{2} a \hat{x} + \frac{1}{2} a \hat{y}, \\ \delta_3 &= -a \hat{y}. \end{aligned}$$



$$t_1 \approx 2.7 \text{ eV}$$

$$(2) \quad \begin{aligned} \hat{H}_{NNN} &= t_2 \sum_{\mathbf{R}} \left(c_{\mathbf{R}+\mathbf{a}_1}^\dagger c_{\mathbf{R}} + c_{\mathbf{R}+\mathbf{a}_2}^\dagger c_{\mathbf{R}} + c_{\mathbf{R}+\mathbf{a}_3}^\dagger c_{\mathbf{R}} \right) \\ &+ t_2 \sum_{\mathbf{R}} \left(d_{\mathbf{R}+\delta_1+\mathbf{a}_1}^\dagger d_{\mathbf{R}+\delta_1} + d_{\mathbf{R}+\delta_1+\mathbf{a}_2}^\dagger d_{\mathbf{R}+\delta_1} \right. \\ &\quad \left. + d_{\mathbf{R}+\delta_1+\mathbf{a}_3}^\dagger d_{\mathbf{R}+\delta_1} \right) + h.c., \end{aligned}$$

$$(3) \quad \hat{H}_{on-site} = \Delta \sum_{\mathbf{R}} c_{\mathbf{R}}^\dagger c_{\mathbf{R}} - \Delta \sum_{\mathbf{R}} d_{\mathbf{R}+\delta_1}^\dagger d_{\mathbf{R}+\delta_1}$$

Fourier
transform

$$c_{\mathbf{R}} = \frac{1}{\sqrt{N}} \sum_{\mathbf{k}} e^{i\mathbf{k}\cdot\mathbf{R}} c_{\mathbf{k}}$$

$$d_{\mathbf{R}+\delta_1} = \frac{1}{\sqrt{N}} \sum_{\mathbf{k}} e^{i\mathbf{k}\cdot(\mathbf{R}+\delta_1)} d_{\mathbf{k}}$$

$$\text{e.g., } \sum_{\mathbf{R}} d_{\mathbf{R}+\delta_1}^\dagger c_{\mathbf{R}} = \frac{1}{N} \sum_{\mathbf{k}, \mathbf{k}'} \sum_{\mathbf{R}} e^{-i(\mathbf{k}'-\mathbf{k})\cdot\mathbf{R}} e^{-i\mathbf{k}'\cdot\delta_1} d_{\mathbf{k}'}^\dagger c_{\mathbf{k}}$$

$$= \sum_{\mathbf{k}} e^{-i\mathbf{k}\cdot\delta_1} d_{\mathbf{k}}^\dagger c_{\mathbf{k}},$$

$$\sum_{\mathbf{R}} e^{i(\mathbf{k}'-\mathbf{k})\cdot\mathbf{R}} = N\delta_{\mathbf{k}'\mathbf{k}}.$$

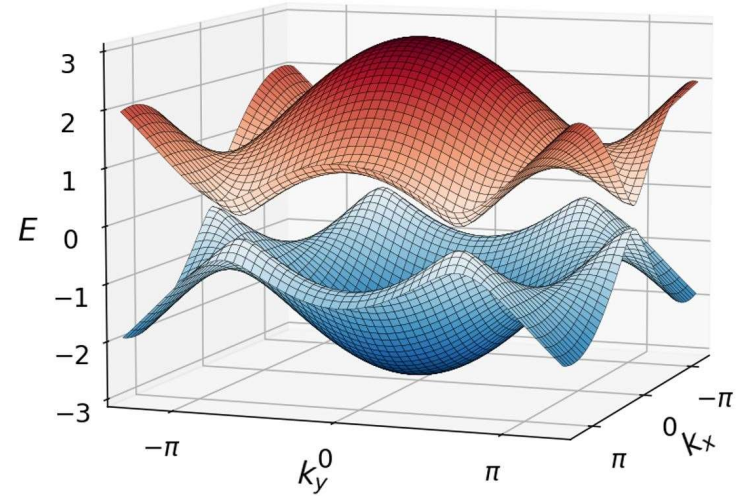
$$\begin{aligned} \Rightarrow \hat{H} &= t_1 \sum_{\mathbf{k}} (e^{-i\mathbf{k}\cdot\delta_1} + e^{-i\mathbf{k}\cdot\delta_2} + e^{-i\mathbf{k}\cdot\delta_3}) d_{\mathbf{k}}^\dagger c_{\mathbf{k}} \\ &+ t_2 \sum_{\mathbf{k}} (e^{-i\mathbf{k}\cdot\mathbf{a}_1} + e^{-i\mathbf{k}\cdot\mathbf{a}_2} + e^{-i\mathbf{k}\cdot\mathbf{a}_3}) c_{\mathbf{k}}^\dagger c_{\mathbf{k}} \\ &+ t_2 \sum_{\mathbf{k}} (e^{-i\mathbf{k}\cdot\mathbf{a}_1} + e^{-i\mathbf{k}\cdot\mathbf{a}_2} + e^{-i\mathbf{k}\cdot\mathbf{a}_3}) d_{\mathbf{k}}^\dagger d_{\mathbf{k}} + h.c. \\ &+ \Delta \sum_{\mathbf{k}} (c_{\mathbf{k}}^\dagger c_{\mathbf{k}} - d_{\mathbf{k}}^\dagger d_{\mathbf{k}}) \\ &= \sum_{\mathbf{k}} \begin{pmatrix} c_{\mathbf{k}}^\dagger & d_{\mathbf{k}}^\dagger \end{pmatrix} H(\mathbf{k}) \begin{pmatrix} c_{\mathbf{k}} \\ d_{\mathbf{k}} \end{pmatrix}. \end{aligned}$$

$$\begin{aligned}
 H(\mathbf{k}) &= \begin{pmatrix} 2t_2 \sum_i \cos \mathbf{k} \cdot \mathbf{a}_i + \Delta & t_1 \sum_i e^{i\mathbf{k} \cdot \boldsymbol{\delta}_i} \\ t_1 \sum_i e^{-i\mathbf{k} \cdot \boldsymbol{\delta}_i} & 2t_2 \sum_i \cos \mathbf{k} \cdot \mathbf{a}_i - \Delta \end{pmatrix} \\
 &= h_0(\mathbf{k}) + \mathbf{h}(\mathbf{k}) \cdot \boldsymbol{\sigma},
 \end{aligned}$$

$$h_0(\mathbf{k}) = 2t_2 \sum_i \cos \mathbf{k} \cdot \mathbf{a}_i,$$

$$\mathbf{h}(\mathbf{k}) = \left(t_1 \sum_i \cos \mathbf{k} \cdot \boldsymbol{\delta}_i, -t_1 \sum_i \sin \mathbf{k} \cdot \boldsymbol{\delta}_i, \Delta \right)$$

$$\varepsilon_{\pm}(\mathbf{k}) = h_0(\mathbf{k}) \pm |\mathbf{h}(\mathbf{k})|$$



$$\begin{aligned}
 |\mathbf{h}| &= \sqrt{3t_1^2 + 2t_1^2 (\cos \mathbf{k} \cdot \mathbf{a}_1 + \cos \mathbf{k} \cdot \mathbf{a}_2 + \cos \mathbf{k} \cdot \mathbf{a}_3) + \Delta^2} \\
 &= \sqrt{3t_1^2 + 2t_1^2 f(\mathbf{k}) + \Delta^2}, \quad t_1 \simeq 2.7 \text{ eV}
 \end{aligned}$$

$$\begin{aligned}
 f(\mathbf{k}) &\equiv \cos \mathbf{k} \cdot \mathbf{a}_1 + \cos \mathbf{k} \cdot \mathbf{a}_2 + \cos \mathbf{k} \cdot \mathbf{a}_3 \\
 &= \cos \sqrt{3}ak_x + 2 \cos \frac{\sqrt{3}}{2}ak_x \cos \frac{3}{2}ak_y.
 \end{aligned}$$

Stability of the nodal point in graphene

- TRS $H(\vec{k})^* = H(-\vec{k})$
 $\rightarrow h_x(\vec{k}), h_y(\vec{k}), h_z(\vec{k}) = \text{even, odd, even}$

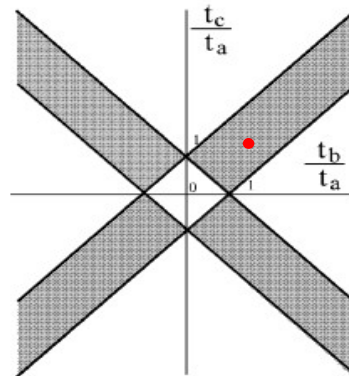
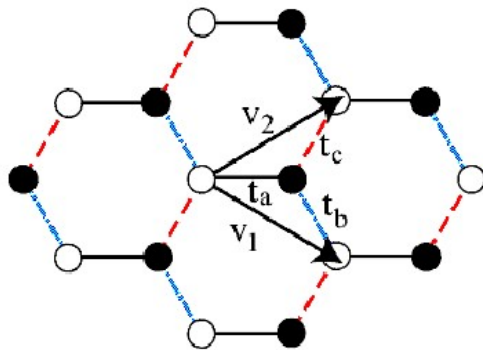
- SIS (for graphene, $\pi = \sigma_x$)

$$\sigma_x H(\vec{k}) \sigma_x = H(-\vec{k})$$

$$\rightarrow h_x(\vec{k}), h_y(\vec{k}), h_z(\vec{k}) = \text{even, odd, odd}$$

- TRS+SIS \rightarrow no σ_z term \leftarrow Co-dimension is 2
 (point degeneracy in 2D BZ)

- Global stability: point degeneracy is further protected by C_3 symmetry
 (Ch7, Bernevig)



Hasegawa et al, PRB 2006

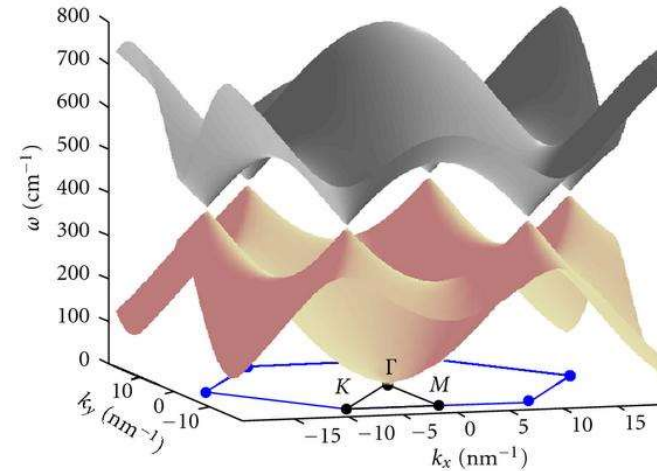
Low-energy effective Hamiltonian near Dirac point

$$\mathbf{K}_1 = \frac{2\pi}{a} \left(\frac{2}{3\sqrt{3}}, 0 \right),$$

$$\mathbf{K}_2 = \frac{2\pi}{a} \left(\frac{1}{3\sqrt{3}}, \frac{1}{3} \right)$$

Alternative:
 $\mathbf{K}_2 = -\mathbf{K}_1$

$$\mathbf{k} = \mathbf{K}_i + \mathbf{k}_i, \quad |\mathbf{k}_i| \ll |\mathbf{K}_i|; \quad i = 1, 2.$$



$$H_{12}(\mathbf{k}) = t_1 \left(e^{i\mathbf{K}_1 \cdot \boldsymbol{\delta}_1} e^{i\mathbf{k}_1 \cdot \boldsymbol{\delta}_1} + e^{i\mathbf{K}_1 \cdot \boldsymbol{\delta}_2} e^{i\mathbf{k}_1 \cdot \boldsymbol{\delta}_2} + e^{i\mathbf{K}_1 \cdot \boldsymbol{\delta}_3} e^{i\mathbf{k}_1 \cdot \boldsymbol{\delta}_3} \right)$$

	$i = 1$	2	3
$\mathbf{K}_1 \cdot \boldsymbol{\delta}_i =$	$+\frac{2\pi}{3}$	$-\frac{2\pi}{3}$	0
$\mathbf{K}_2 \cdot \boldsymbol{\delta}_i =$	$-\frac{2\pi}{3}$	$+\frac{2\pi}{3}$	0
$e^{i\mathbf{K}_{1/2} \cdot \boldsymbol{\delta}_i} =$	$-\frac{1}{2} \pm \frac{\sqrt{3}}{2}i$	$-\frac{1}{2} \mp \frac{\sqrt{3}}{2}i$	1

(rewrite $k_{1,2}$ simply as k)

$$\begin{aligned} \Rightarrow H_{12}(\mathbf{k}) &\simeq it_1 a \mathbf{k} \cdot \left(\pm \frac{3}{2}i, -\frac{3}{2} \right) \\ &= t_1 a \left(\mp \frac{3}{2} k_x - \frac{3}{2} i k_y \right) \end{aligned}$$

$$\begin{aligned} \mathbf{H}(\mathbf{k}) &\simeq \begin{pmatrix} \Delta & \frac{3}{2} t_1 a (\mp k_x - i k_y) \\ \frac{3}{2} t_1 a (\mp k_x + i k_y) & -\Delta \end{pmatrix} \\ &= \hbar v_F (\tau k_x \sigma_x + k_y \sigma_y) + \Delta \sigma_z, \end{aligned}$$

↑ valley

$$v_F = \frac{\frac{3}{2} a t_1}{\hbar} \simeq \frac{c}{300}$$

Near K_2 -valley

$$H = \hbar v_F \vec{\sigma} \cdot (\vec{k} - \vec{K}_2)$$

Under time-reversal, $K_2 \rightarrow -K_2 = K_1$

$$H \longrightarrow H' = \hbar v_F \vec{\sigma}^* \cdot (-\vec{k} - \vec{K}_2) = -\hbar v_F \vec{\sigma}^* \cdot (\vec{k} - \vec{K}_1)$$

As a result, the **Berry curvature** and **orbital magnetization** at K and $-K$ are opposite in signs

- Effective Hamiltonian near degenerate point

$$H_0 = \hbar v_F (\mp k_x \sigma_x + k_y \sigma_y) + \Delta \sigma_z \text{ at } \pm K, \quad \hbar v_F \equiv \frac{3}{2} t_1 a$$

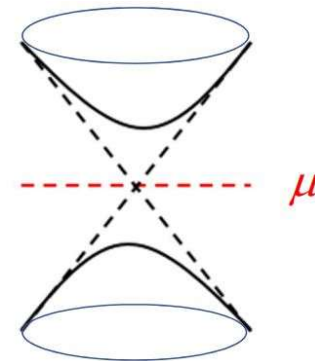
- Berry curvature

$$F_{z\tau}^{\pm}(\mathbf{k}) = \pm \tau \frac{1}{2} \frac{\hbar^2 v_F^2 \Delta}{\hbar^3}$$

$$\int_{all} d^2k F_{\tau}^{\pm} = \pm \tau \pi \quad (\text{Drop sub } z)$$

$$\rightarrow \sigma_H = \frac{e^2}{h} \frac{1}{2\pi} \int d^2k F_{\tau}^{-} = -\frac{\tau e^2}{2h}$$

Total Hall conductivity is zero due to the cancellation between 2 valleys.

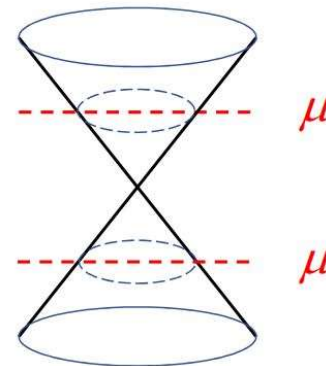


- Gapless limit (at $+K$):

$$\rightarrow \text{Berry phase (surrounding } +K): \gamma_C = \mp \pi$$

Berry phase remains the same

$$\rightarrow F^{\pm}(\vec{k}) = \mp \pi \delta^2(\vec{k})$$



Graphene in magnetic field

Bohr-Sommerfeld quantization (Kittel)

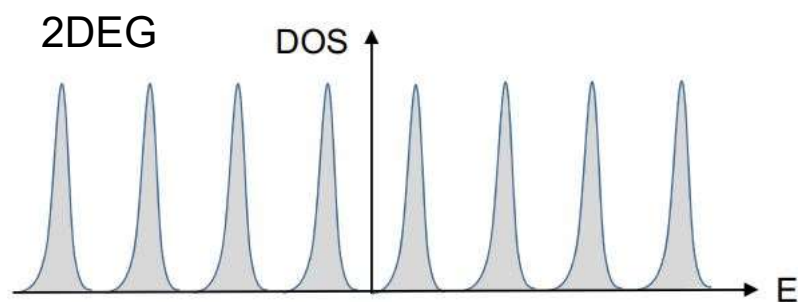
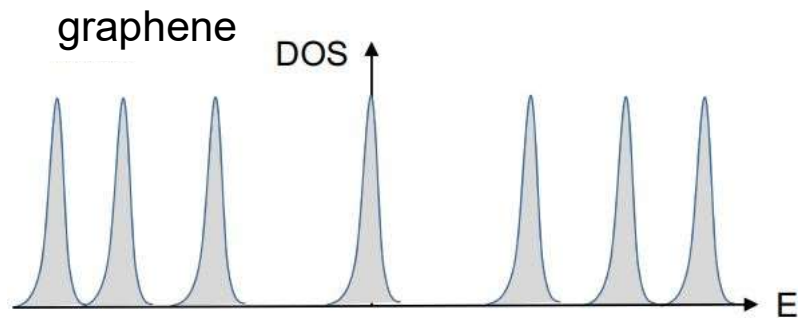
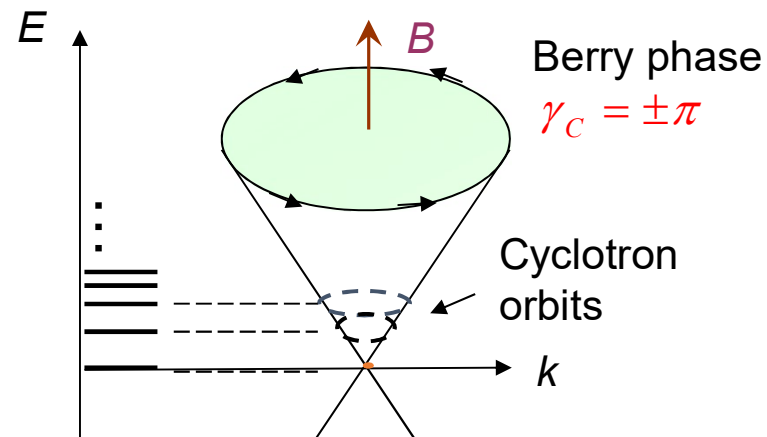
$$\underbrace{\frac{1}{2} \oint_C (\vec{k} \times d\vec{k}) \cdot \hat{z}}_{\text{Orbital area}} = 2\pi \left(n + \frac{1}{2} - \frac{\gamma_C}{2\pi} \right) \frac{eB}{\hbar}$$

Correction from Berry phase

→ $\pi k^2 = 2\pi \left(n + \frac{1}{2} - \frac{\gamma_C}{2\pi} \right) \frac{eB}{\hbar}$

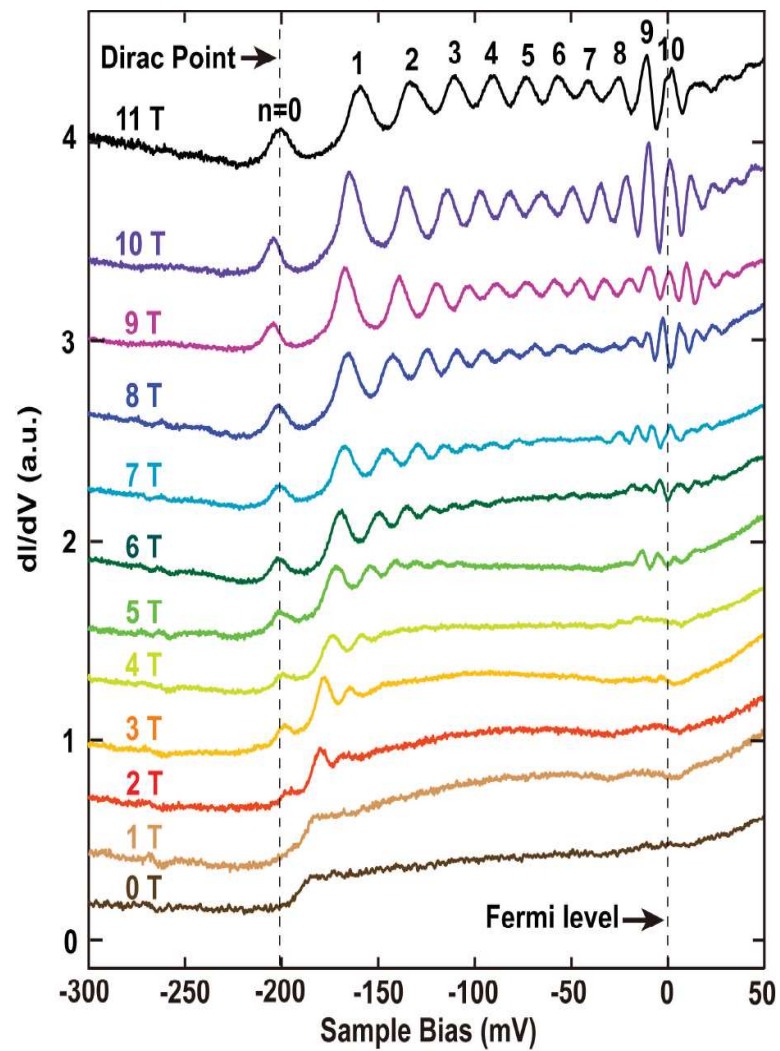
$$E(k) = \hbar v_F k$$

→ $E_n = v_F \sqrt{2eB\hbar n}$ Landau levels

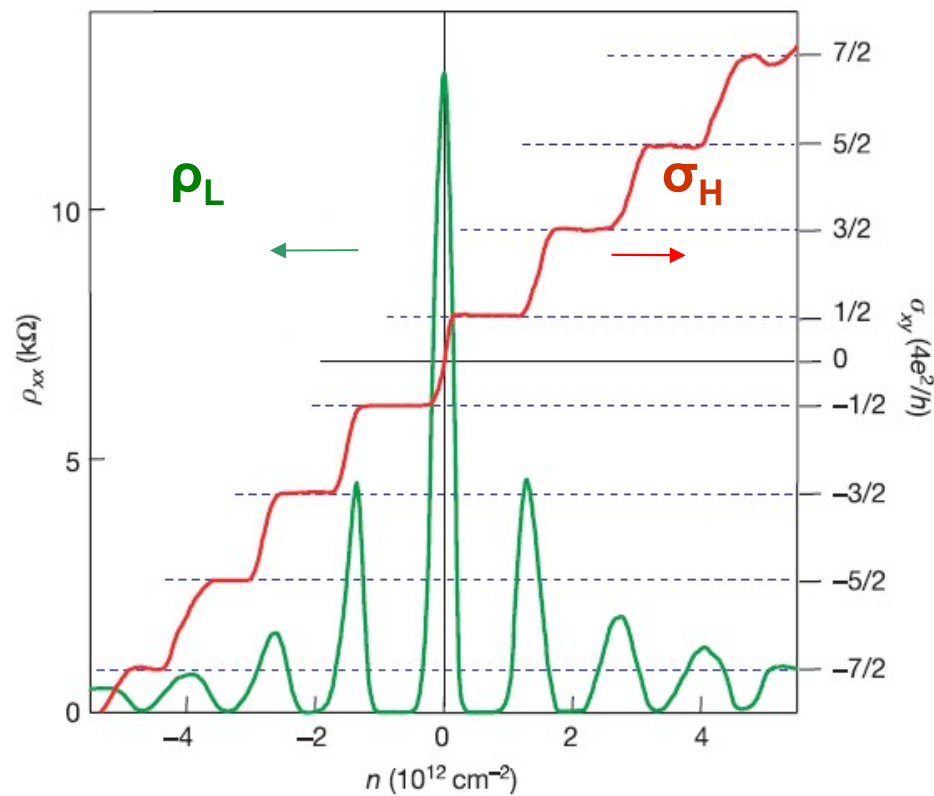


STM experiment

(Cheng et al, PRL 2010)

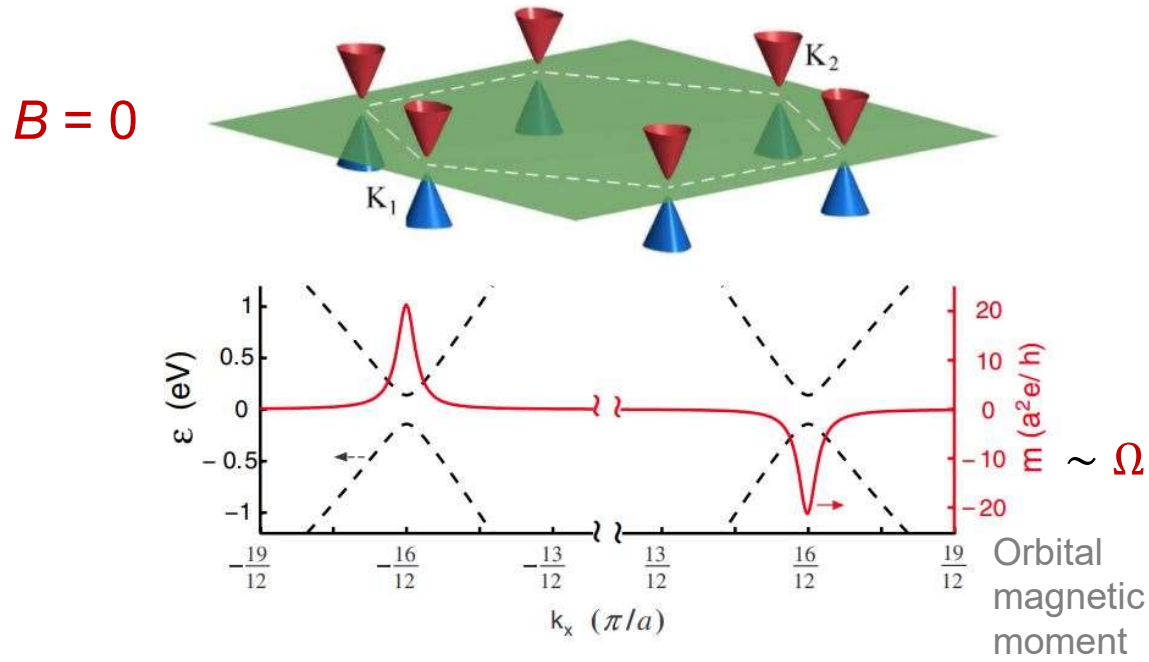


Quantum Hall effect in graphene



Novoselov et al, Nature 2005

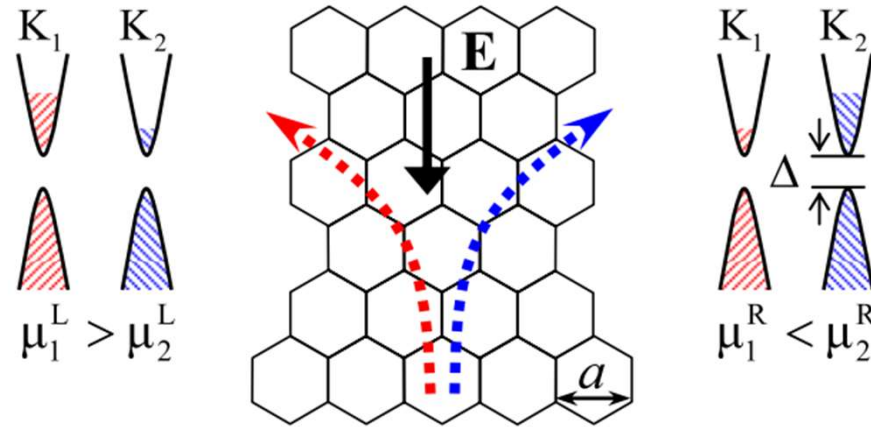
Valley Hall effect (Xiao et al, PRL 2007)



Opposite anomalous velocities

from two valleys

$$\mathbf{v}_n(\mathbf{k}) = \frac{1}{\hbar} \frac{\partial \varepsilon_{n\mathbf{k}}}{\partial \mathbf{k}} + \frac{e}{\hbar} \mathbf{E} \times \mathbf{F}_n(\mathbf{k})$$

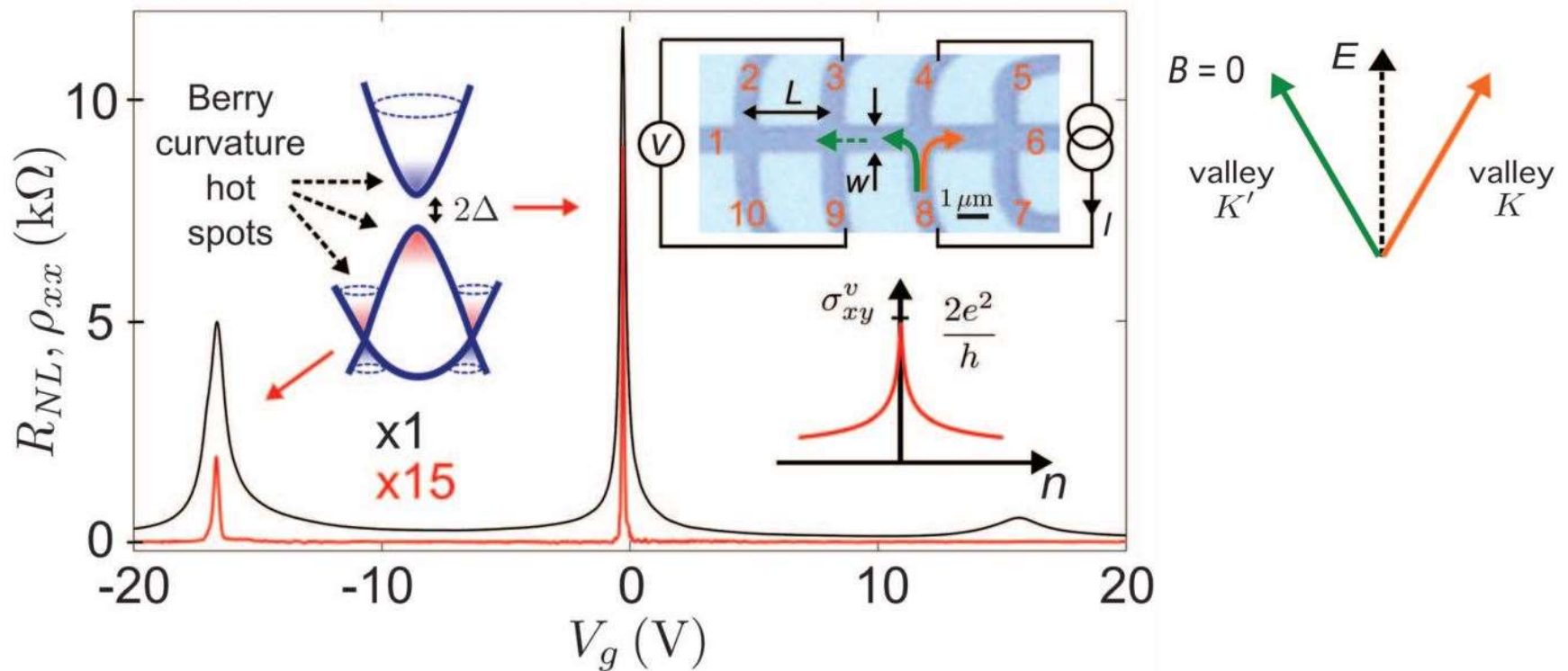


Detecting topological currents in graphene superlattices

Science, 2014

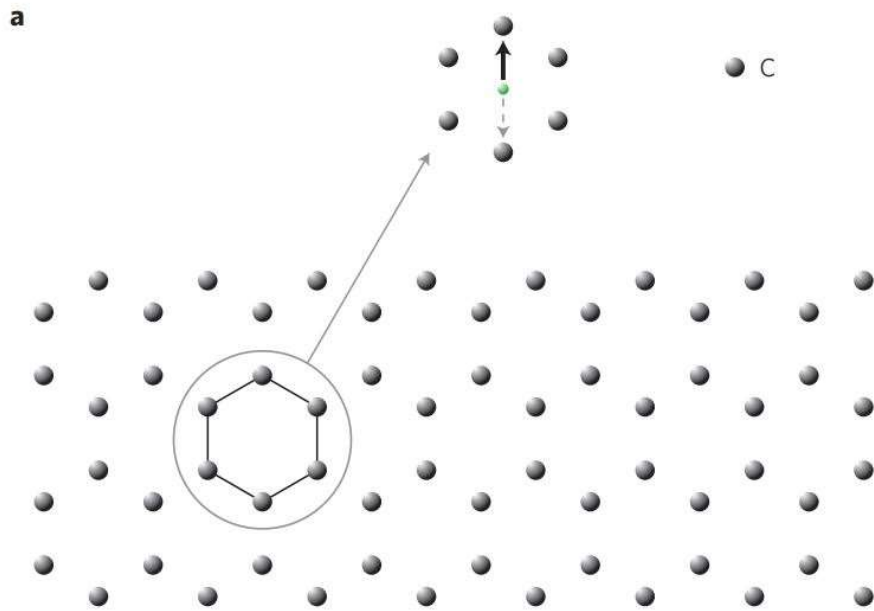
R. V. Gorbachev,^{1,2*} J. C. W. Song,^{3,4*} G. L. Yu,¹ A. V. Kretinin,² F. Withers,² Y. Cao,¹
 A. Mishchenko,¹ I. V. Grigorieva,² K. S. Novoselov,² L. S. Levitov,^{3*} A. K. Geim^{1,2†}

Graphene on hBN (breaking inversion symm $\rightarrow 2\Delta = 30$ meV)



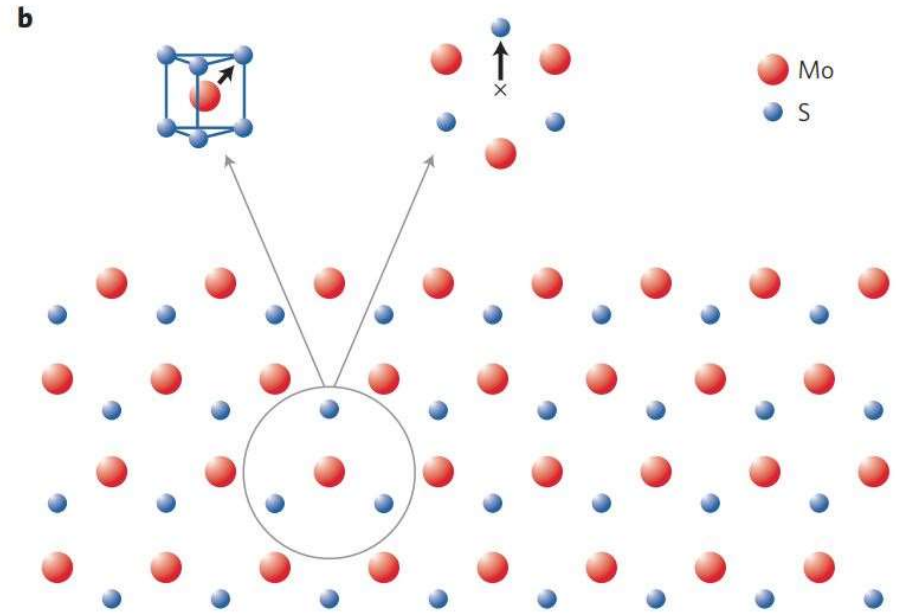
2D material: graphene, silicene, hBN, TMD ...e6c

Graphene (with SIS)



Graphene on hBN breaks SIS,
opens a gap ~ 30 mV

monolayer MoS₂ (without SIS)



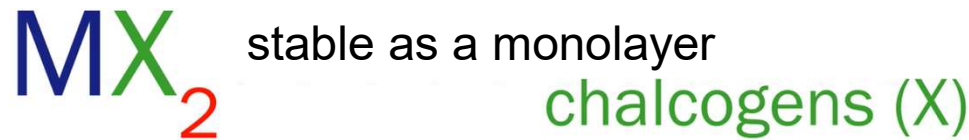
An energy gap ~ 1.9 eV
(easier for optical and electrical control)

2 Transition Metal Dichalcogenide (TMD)

硫族化物 **chalcogens (X)**

hydrogen 1 H 1.0079																	helium 2 He 4.0026	
lithium 3 Li 6.941	beryllium 4 Be 9.0122																	neon 10 Ne 20.180
sodium 11 Na 22.990	magnesium 12 Mg 24.305																	argon 18 Ar 39.948
potassium 19 K 39.098	calcium 20 Ca 40.078	scandium 21 Sc 44.956	titanium 22 Ti 47.887	vanadium 23 V 50.942	chromium 24 Cr 51.996	manganese 25 Mn 54.938	iron 26 Fe 55.845	cobalt 27 Co 58.933	nickel 28 Ni 58.693	copper 29 Cu 63.546	zinc 30 Zn 65.39	gallium 31 Ga 69.723	germanium 32 Ge 72.61	arsenic 33 As 74.922	selenium 34 Se 78.96	bromine 35 Br 79.904	krypton 36 Kr 83.80	
rubidium 37 Rb 85.468	strontium 38 Sr 87.62	yttrium 39 Y 88.906	zirconium 40 Zr 91.224	niobium 41 Nb 92.906	molybdenum 42 Mo 95.94	technetium 43 Tc 98	ruthenium 44 Ru 101.07	rhodium 45 Rh 102.91	palladium 46 Pd 106.42	silver 47 Ag 107.87	cadmium 48 Cd 112.41	indium 49 In 114.82	tin 50 Sn 118.71	antimony 51 Sb 121.75	tellurium 52 Te 127.6	iodine 53 I 126.90	xenon 54 Xe 131.29	
cesium 55 Cs 132.91	barium 56 Ba 137.33	* 57-70	lanthanum 57 Lu 174.97	hafnium 72 Hf 178.49	tantalum 73 Ta 180.95	wolfram 74 W 183.84	reuterium 75 Re 186.21	osmium 76 Os 190.23	iridium 77 Ir 192.22	platinum 78 Pt 195.08	gold 79 Au 196.97	mercury 80 Hg 200.59	thallium 81 Tl 203.38	lead 82 Pb 207.2	bismuth 83 Bi 208.98	polonium 84 Po 209	astatine 85 At 210	radon 86 Rn 222
francium 87 Fr [223]	radium 88 Ra [226]	* * 89-102	actinium 89 Ac [227]	thorium 90 Th [232]	protactinium 91 Pa [231]	uranium 92 U [238]	neptunium 93 Np [237]	plutonium 94 Pu [244]	americium 95 Am [243]	curium 96 Cm [247]	berkelium 97 Bk [247]	californium 98 Cf [251]	lawrencium 99 Lr [260]	unlabeled 100 Uun [261]	unlabeled 101 Uuu [262]	unlabeled 102 Uub [263]	unlabeled 103 Uuc [264]	unlabeled 104 Uud [265]

transition metals (M)



hydrogen 1 H 1.0079																	helium 2 He 4.0026	
lithium 3 Li 6.941	beryllium 4 Be 9.0122																	neon 10 Ne 20.180
sodium 11 Na 22.990	magnesium 12 Mg 24.305																	argon 18 Ar 39.948
potassium 19 K 39.098	calcium 20 Ca 40.078	scandium 21 Sc 44.956	titanium 22 Ti 47.887	vanadium 23 V 50.942	chromium 24 Cr 51.996	manganese 25 Mn 54.938	iron 26 Fe 55.845	cobalt 27 Co 58.933	nickel 28 Ni 58.693	copper 29 Cu 63.546	zinc 30 Zn 65.39	gallium 31 Ga 69.723	germanium 32 Ge 72.61	arsenic 33 As 74.922	selenium 34 Se 78.96	bromine 35 Br 79.904	krypton 36 Kr 83.80	
rubidium 37 Rb 85.468	strontium 38 Sr 87.62	yttrium 39 Y 88.906	zirconium 40 Zr 91.224	niobium 41 Nb 92.906	molybdenum 42 Mo 95.94	technetium 43 Tc 98	ruthenium 44 Ru 101.07	rhodium 45 Rh 102.91	palladium 46 Pd 106.42	silver 47 Ag 107.87	cadmium 48 Cd 112.41	indium 49 In 114.82	tin 50 Sn 118.71	antimony 51 Sb 121.75	tellurium 52 Te 127.6	iodine 53 I 126.90	xenon 54 Xe 131.29	
cesium 55 Cs 132.91	barium 56 Ba 137.33	* 57-70	lanthanum 57 Lu 174.97	hafnium 72 Hf 178.49	tantalum 73 Ta 180.95	wolfram 74 W 183.84	reuterium 75 Re 186.21	osmium 76 Os 190.23	iridium 77 Ir 192.22	platinum 78 Pt 195.08	gold 79 Au 196.97	mercury 80 Hg 200.59	thallium 81 Tl 203.38	lead 82 Pb 207.2	bismuth 83 Bi 208.98	polonium 84 Po 209	astatine 85 At 210	radon 86 Rn 222
francium 87 Fr [223]	radium 88 Ra [226]	* * 89-102	actinium 89 Ac [227]	thorium 90 Th [232]	protactinium 91 Pa [231]	uranium 92 U [238]	neptunium 93 Np [237]	plutonium 94 Pu [244]	americium 95 Am [243]	curium 96 Cm [247]	berkelium 97 Bk [247]	californium 98 Cf [251]	lawrencium 99 Lr [260]	unlabeled 100 Uun [261]	unlabeled 101 Uuu [262]	unlabeled 102 Uub [263]	unlabeled 103 Uuc [264]	unlabeled 104 Uud [265]

transition metals (M)

3 possible forms of MX_2 :

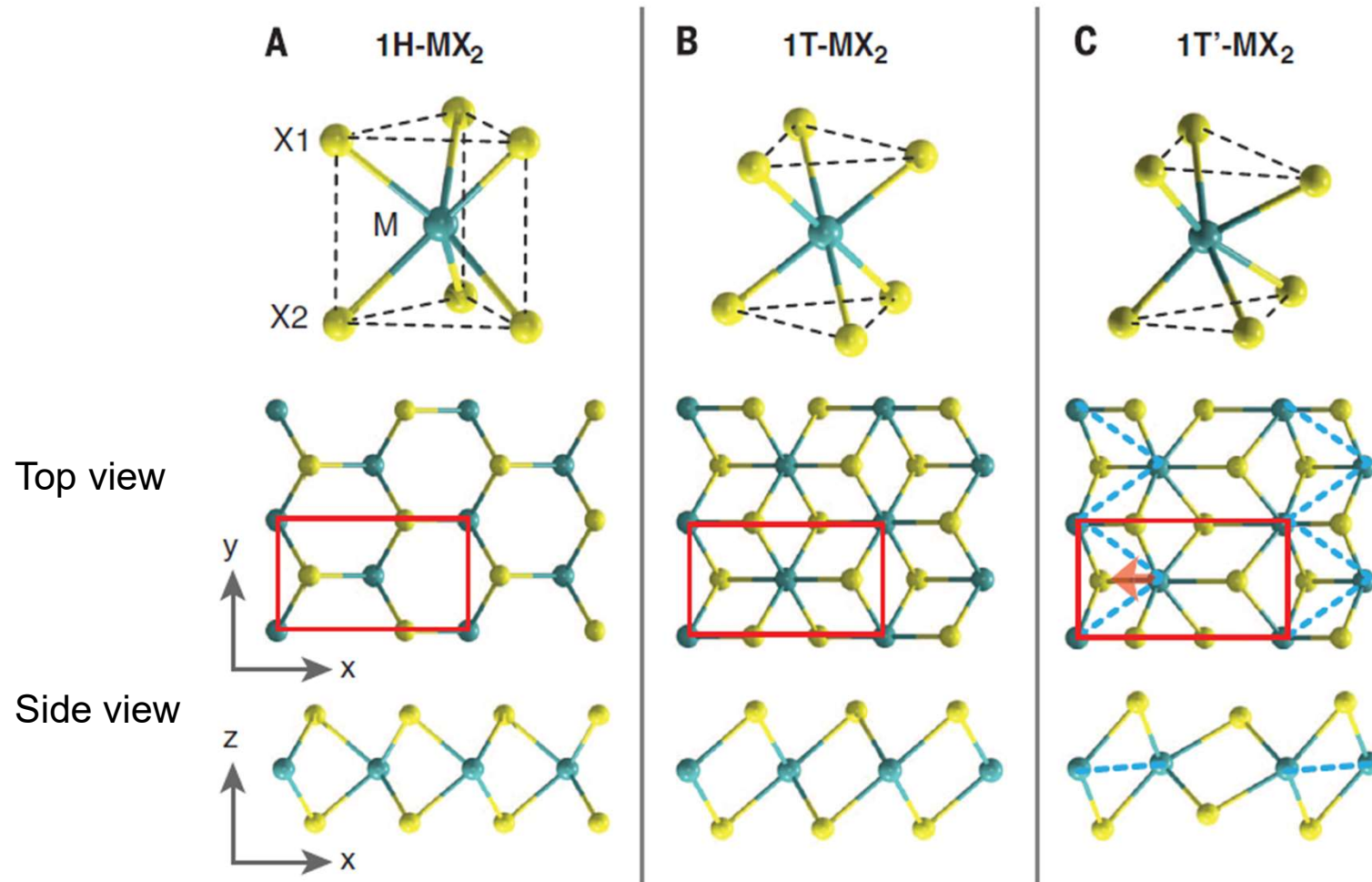
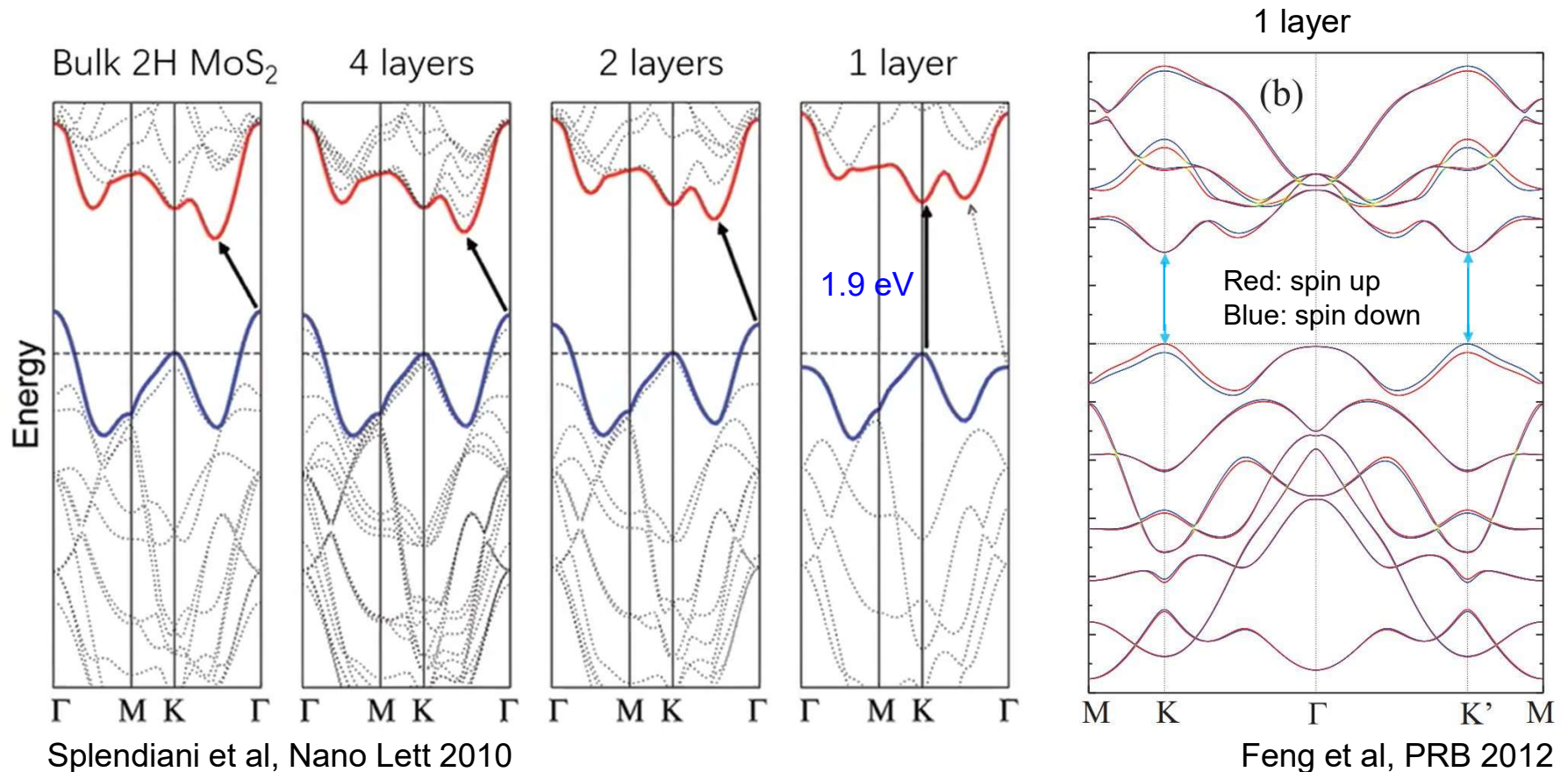


Fig from Qian et al, Science 2014

Transition Metal Dichalcogenide: MoS₂

- Bulk indirect band gap (with SIS); single layer **direct band gap** (without SIS)
- Massive Dirac fermion
- **Large SO coupling, spin-valley locking** (due to Kramer degeneracy)
- Room temperature mobility 3-4 order of magnitude lower than in graphene
- Strong Coulomb interaction, excitons



Massive Dirac points of MoS₂ monolayer

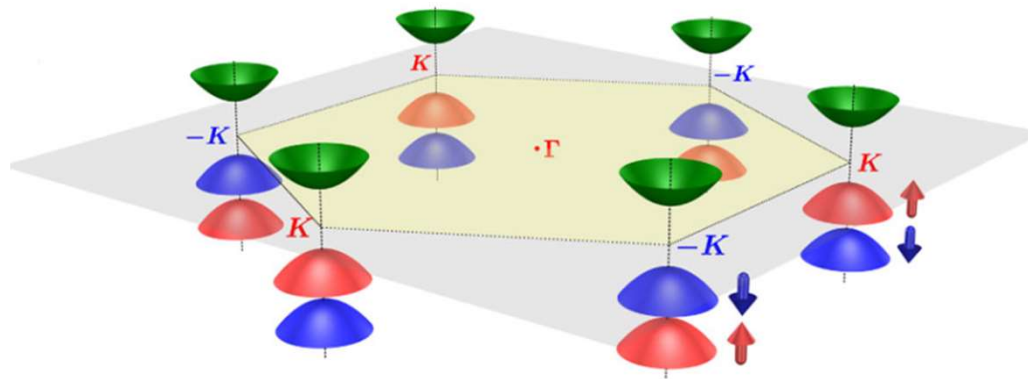


Fig from Xiao et al, PRL 2012

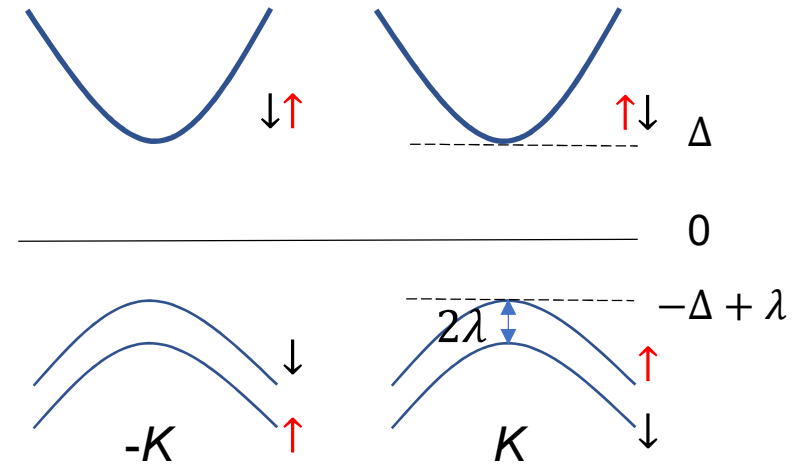
Effective 2-band model near Dirac points

$$H = \alpha(\tau k_x \sigma_x + k_y \sigma_y) + \Delta' \sigma_z + \frac{\lambda}{2}$$

$$\Delta' \equiv \Delta - \lambda/2$$

$$\varepsilon_k^{c/v} = \pm \sqrt{\alpha^2 k^2 + \Delta'^2} + \frac{\lambda}{2}$$

Berry curvature



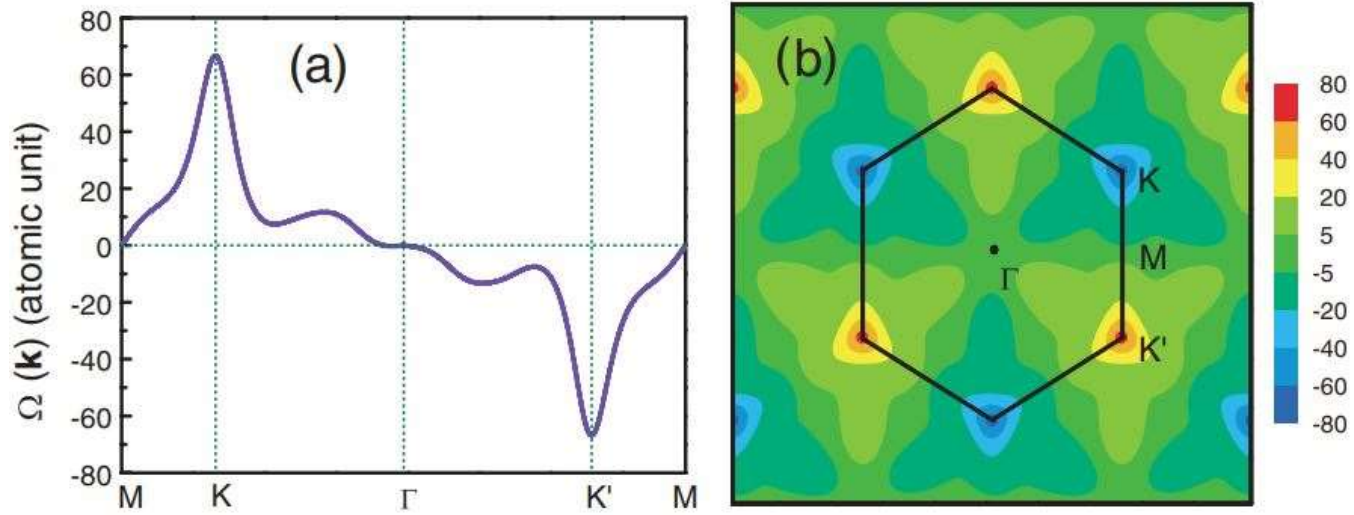
$$F_c^\tau(\mathbf{k}) = \frac{\tau}{2} \frac{\alpha^2 \Delta'}{[\alpha^2 k^2 + \Delta'^2]^{3/2}}$$

Opposite valleys have opposite BCs

For partially-filled valence band,

$$\begin{aligned} \sigma_H^\tau &= \frac{1}{2\pi} \int d^2 k F_c^\tau(\mathbf{k}) \\ &= \frac{\tau}{2} \left[1 - \frac{\Delta'}{\sqrt{\alpha^2 k_F^2 + \Delta'^2}} \right] \end{aligned}$$

The Berry curvatures of monolayer MoS₂

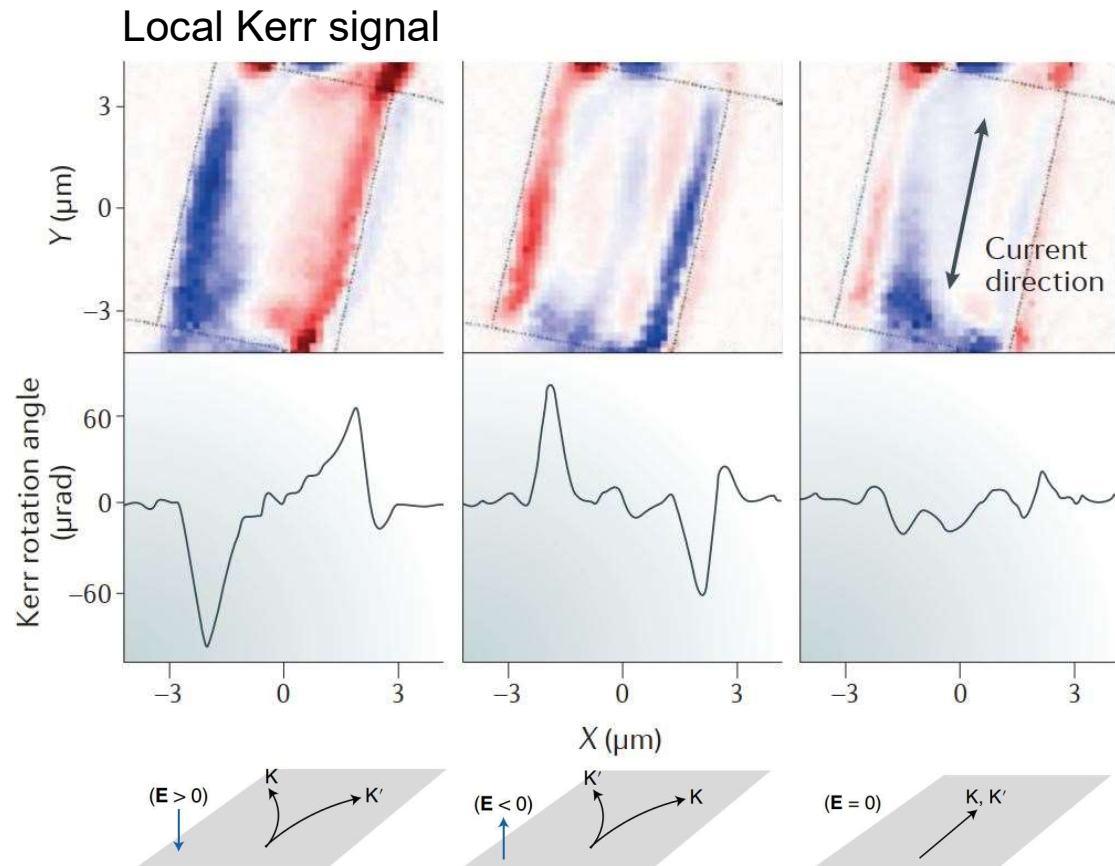


Feng et al, PRB 2012

The valley Hall effect in MoS₂ transistors

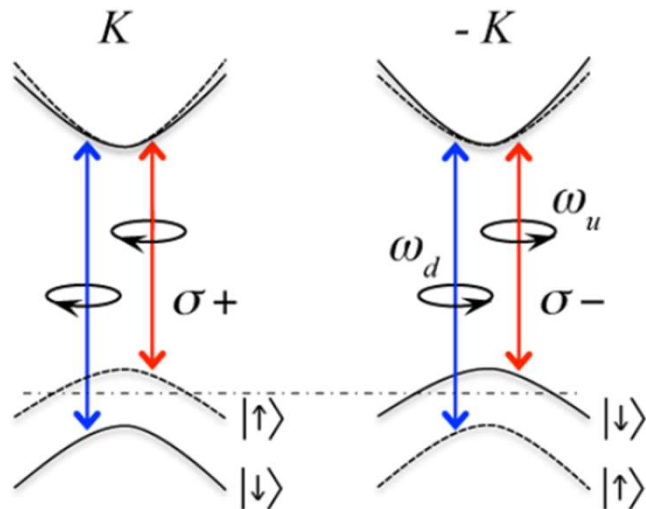
K. F. Mak,^{1,2*} K. L. McGill,² J. Park,^{1,3} P. L. McEuen^{1,2*}

Lee et al, Nature Nano Tech, 2016
Bilayer MoS₂ with SIS (broken by E field)

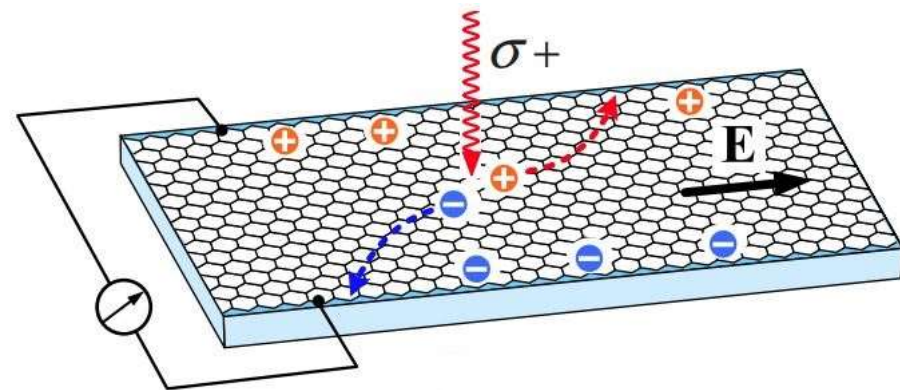


Valley-selective optical pumping
(Yao et al, PRB 2008)

- K, K' population imbalance induced by optical pumping
→ photo-induced AHE



Optical field couples only to the orbital part of the wave function and spin is conserved in the optical transitions.



Solid circles: electrons - and holes + in K -valley. The currents add up.

Two-dimensional material

- 1 • Graphene
 - symmetries
 - Effective Hamiltonian
- 2 • Transition metal dichalcogenide
 - Berry curvature
 - Optical transitions
- 3 • Haldane model
 - Haldane flux
 - Berry curvature
- 4 • Twisted bilayer graphene

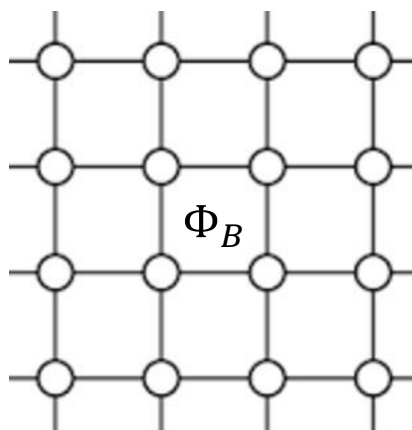
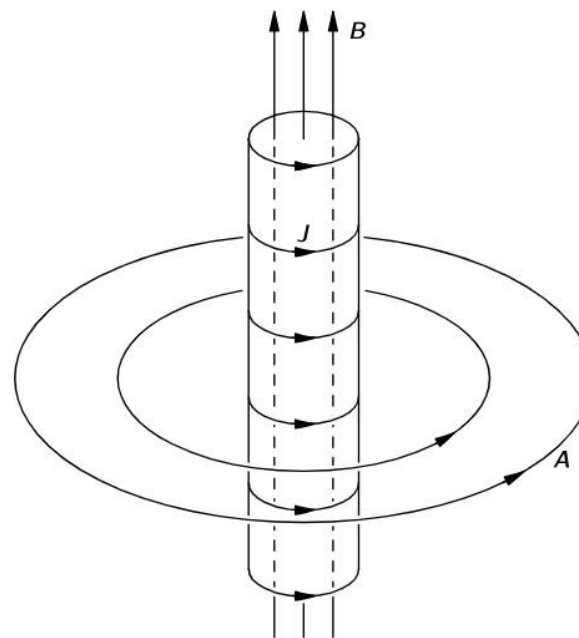
First, electron hopping in a magnetic field

- Aharonov-Bohm (AB) phase

For a closed loop C,

$$\psi' = e^{i\frac{e}{\hbar} \oint_C d\vec{r} \cdot \vec{A}} \psi = e^{2\pi i \frac{\Phi_B}{\Phi_0}}, \quad \Phi_0 \equiv h/e$$

- AB phase and electron hopping



3 Haldane's graphene model, PRL 1989
(no net magnetic field, but TRS is broken)

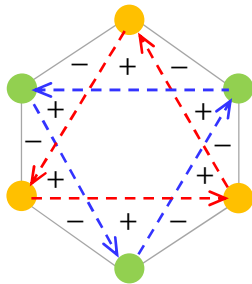
$$H = -t_1 \sum_{\langle i,j \rangle} c_i^\dagger c_j + \Delta \sum_i \xi_i c_i^\dagger c_i + t_2 \sum_{\langle\langle i,j \rangle\rangle} e^{i v_{ij} \phi} c_i^\dagger c_j \quad \text{NNN}$$

\wedge break SIS \wedge break TRS

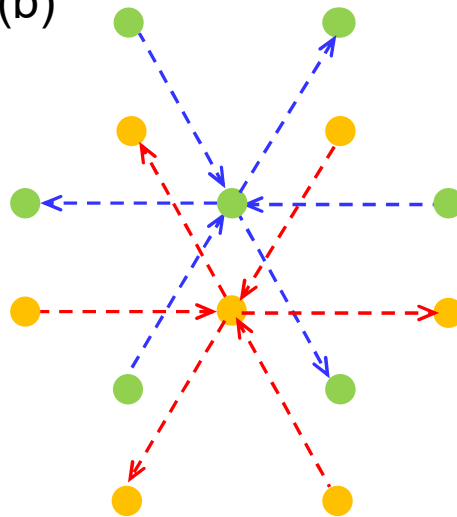
As a result of
Haldane flux

$$\begin{aligned} \mathbf{R}_A &\rightarrow \mathbf{R}_A + \mathbf{a}_i \text{ get } e^{-i\phi}, \quad i = 1, 2, 3 \\ \mathbf{R}_A &\rightarrow \mathbf{R}_A - \mathbf{a}_i \text{ get } e^{+i\phi}, \\ \mathbf{R}_B &\rightarrow \mathbf{R}_A + \mathbf{a}_i \text{ get } e^{+i\phi}, \\ \mathbf{R}_B &\rightarrow \mathbf{R}_A - \mathbf{a}_i \text{ get } e^{-i\phi}. \end{aligned}$$

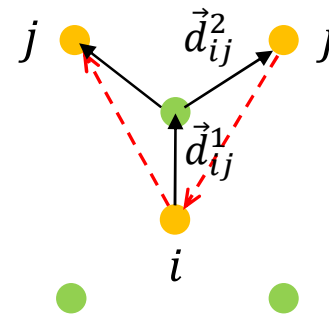
(a)



(b)



(c)



$$v_{ij} \equiv \text{sign}(\hat{d}_{ij}^1 \times \hat{d}_{ij}^2)_z$$

NNN coupling

$$\hat{H}_{NNN} = t_2 \sum_{\mathbf{R}} \sum_{i=1}^3 \left(c_{\mathbf{R}+\mathbf{a}_i}^\dagger c_{\mathbf{R}} e^{-i\phi} + h.c. \right) \\ + t_2 \sum_{\mathbf{R}} \sum_{i=1}^3 \left(d_{\mathbf{R}+\mathbf{a}_i}^\dagger d_{\mathbf{R}} e^{+i\phi} + h.c. \right).$$

$$= 2t_2 \sum_{\mathbf{k}} \sum_i \left[\cos(\mathbf{k} \cdot \mathbf{a}_i + \phi) c_{\mathbf{k}}^\dagger c_{\mathbf{k}} + \cos(\mathbf{k} \cdot \mathbf{a}_i - \phi) d_{\mathbf{k}}^\dagger d_{\mathbf{k}} \right]$$

$$= \sum_{\mathbf{k}} \left(c_{\mathbf{k}}^\dagger, d_{\mathbf{k}}^\dagger \right) \mathbf{H}_{NNN}(\mathbf{k}) \begin{pmatrix} c_{\mathbf{k}} \\ d_{\mathbf{k}} \end{pmatrix}$$

$$\mathbf{H}_{NNN}(\mathbf{k}) = 2t_2 \begin{pmatrix} \sum_i \cos(\mathbf{k} \cdot \mathbf{a}_i + \phi) & 0 \\ 0 & \sum_i \cos(\mathbf{k} \cdot \mathbf{a}_i - \phi) \end{pmatrix}$$

➔ $\mathbf{H}(\mathbf{k}) = \frac{h_{11} + h_{22}}{2} + \mathbf{h} \cdot \boldsymbol{\sigma}$

$$\mathbf{h} = \left(t_1 \sum_i \cos \mathbf{k} \cdot \boldsymbol{\delta}_i, -t_1 \sum_i \sin \mathbf{k} \cdot \boldsymbol{\delta}_i, \frac{h_{11} - h_{22}}{2} + \Delta \right)$$

$$= \underline{-2t_2 \sum_i \sin \mathbf{k} \cdot \mathbf{a}_i \sin \phi} + \Delta$$

Near Dirac point

$$h_3(\mathbf{k}) = \pm 3\sqrt{3}t_2 \sin \phi + \Delta + O(k^2).$$

let $h_3 = m_\tau(\phi, \Delta)$ a ϕ -dependent effective mass

$$\rightarrow H_\tau(\mathbf{k}) = \frac{h_{11} + h_{22}}{2} + \begin{pmatrix} m_\tau & \hbar v_F(\tau k_x - ik_y) \\ \hbar v_F(\tau k_x + ik_y) & -m_\tau \end{pmatrix}$$

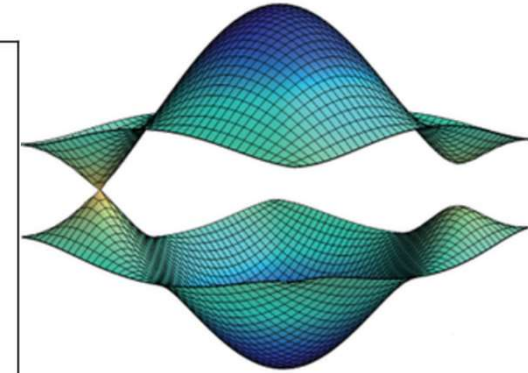
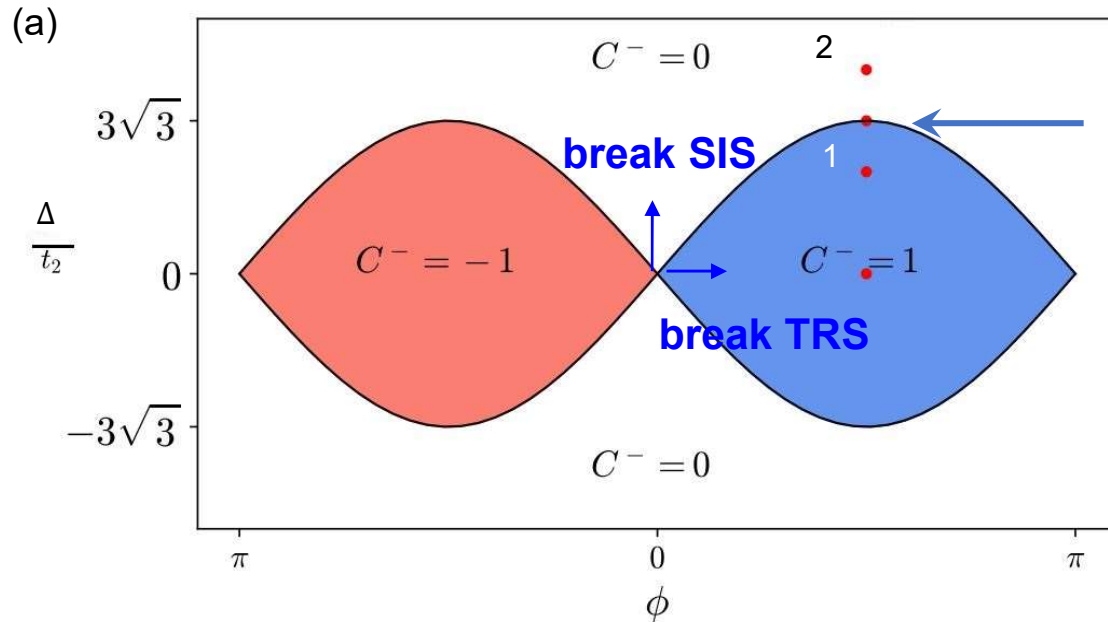
$$F_{z\tau}^+(\mathbf{k}) = \frac{\tau}{2} \frac{\hbar^2 v_F^2 m_\tau}{(\hbar^2 v_F^2 k^2 + m_\tau^2)^{3/2}}$$

The Dirac gap is closed when

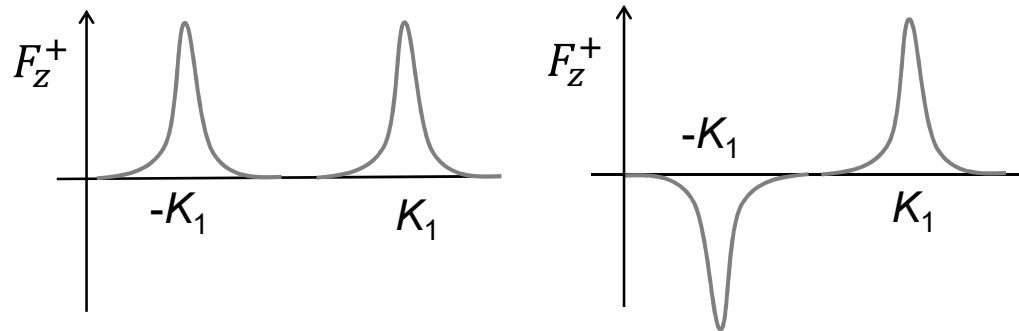
$$m_\pm(\phi, \Delta) = \pm 3\sqrt{3}t_2 \sin \phi + \Delta = 0$$

Phase diagram Zero-field quantum Hall effect phases ($\nu = \pm 1$, where $\sigma^{xy} = \nu e^2/h$) occur if $|M/t_2| < 3\sqrt{3}|\sin\phi|$.

Fig from Atteia's thesis, 2018

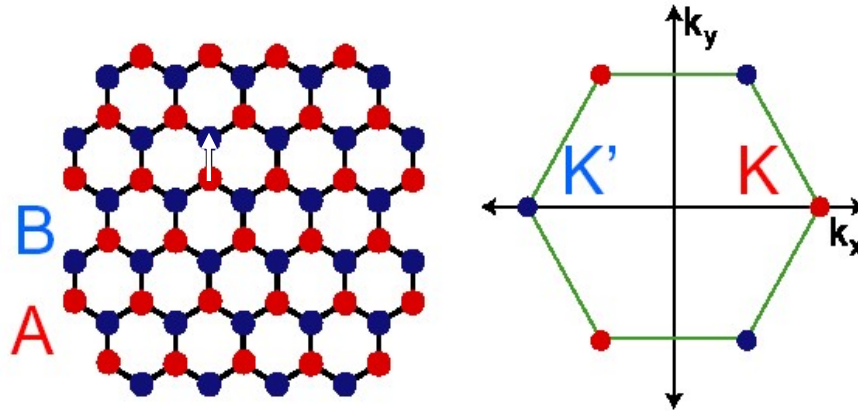


(b) Berry curvatures of point 1 (left) and 2 (right)



3' Kane-Mele model = 2 copies of Haldane model
 (Kane and Mele, PRL 2005)

The first example
 of topological
 insulator



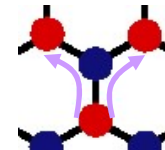
$$H = -t \sum_{\langle i,j \rangle} c_i^\dagger c_j$$

Sublattice potential $+ \lambda_{sub} \sum_i \xi_i c_i^\dagger c_i$

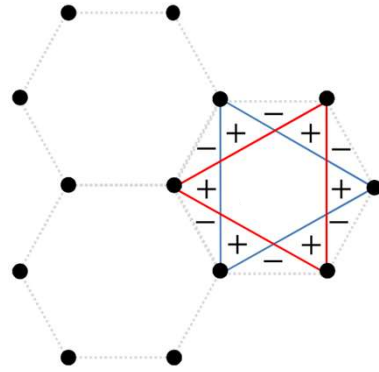
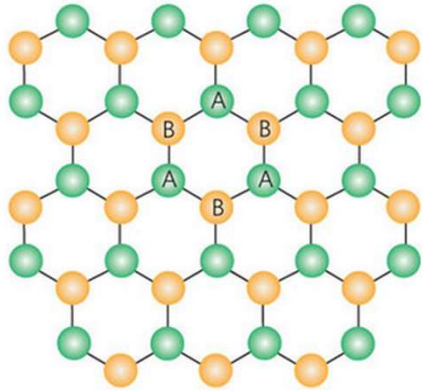
Intrinsic SO coupling $+ i \lambda_{so} \sum_{\langle\langle i,j \rangle\rangle} v_{ij} c_i^\dagger s_z c_j$

$$c_i = \begin{pmatrix} a_{i\uparrow} \\ a_{i\downarrow} \\ b_{i\uparrow} \\ b_{i\downarrow} \end{pmatrix}$$

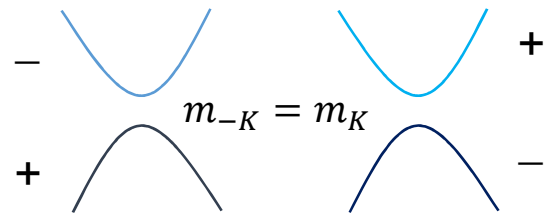
Graphene:
 $\sim L_z S_z \sim 10^{-3} meV$



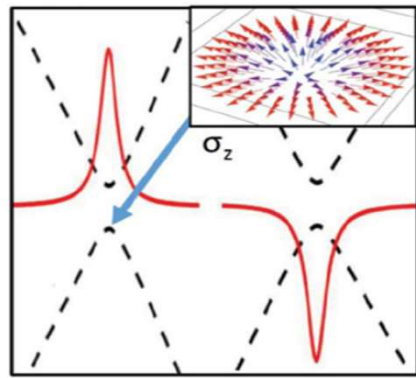
- All of the terms respect TR symm
- H_{sub} breaks space inversion symm
- H_{so} does not break TRS or SIS



• **Semenoff mass** (PRL 1984)

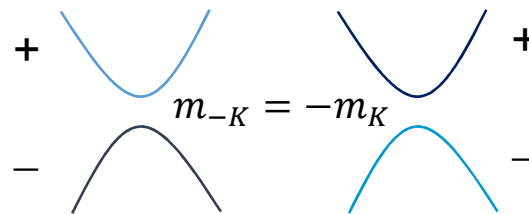


$$H^{\pm K} = H_0 + m\sigma_z$$

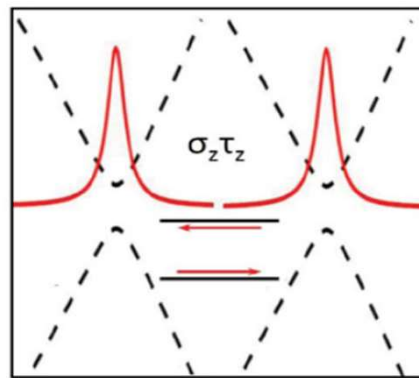


$$\sigma_H = 0$$

• **Haldane mass** (PRL 1989)



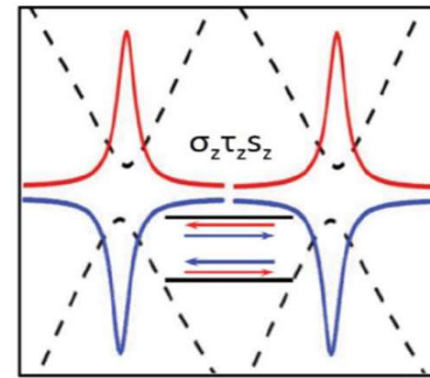
$$H^{\pm K} = H_0 \pm m\sigma_z$$



$$\sigma_H = e^2/h \quad (\text{QAHE})$$

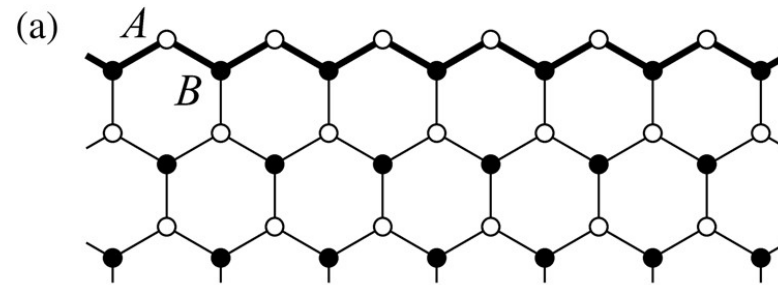
• **Kane-Mele mass** (PRL 2005)

~ 2 copies of Haldane model

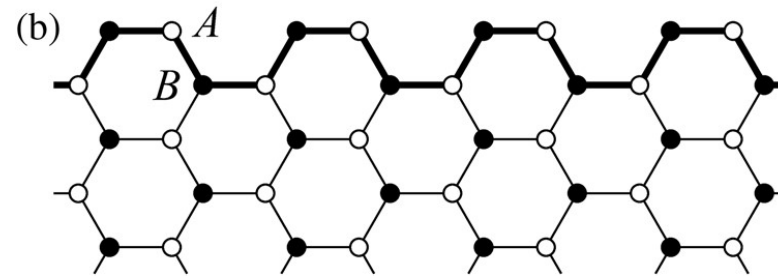


QSHE

Graphene with edge (no topology)

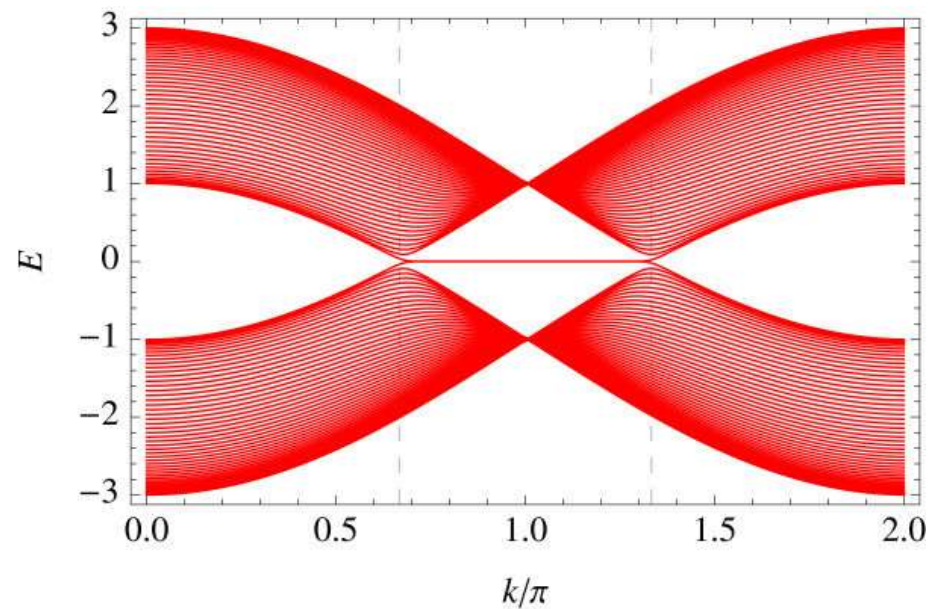


Zigzag edge

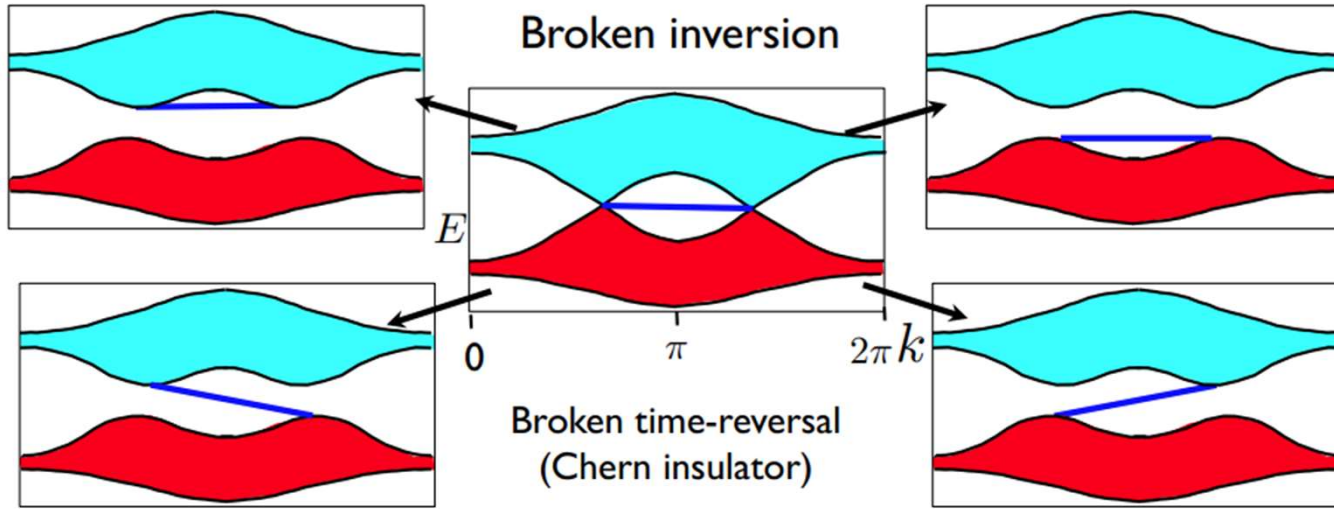


Armchair edge

Edge states for zigzag edge (Fujita, 1996)

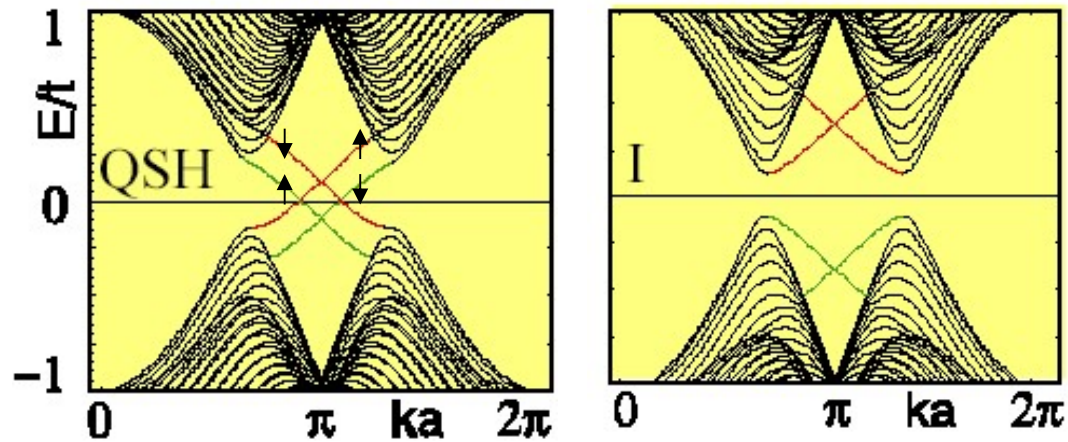


Edge state in different graphene models (for zigzag edge)

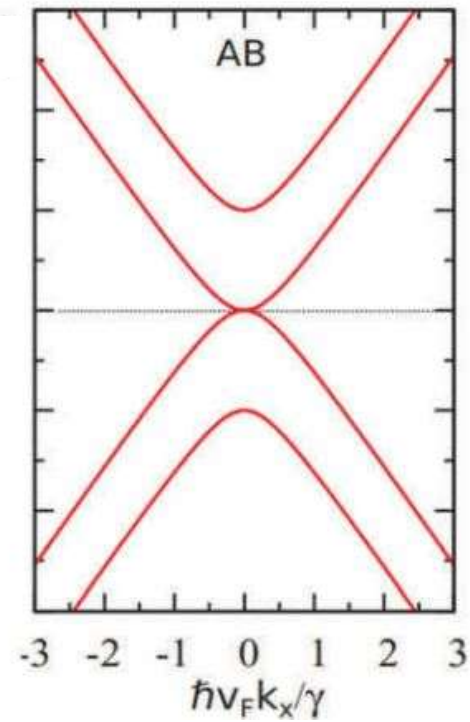
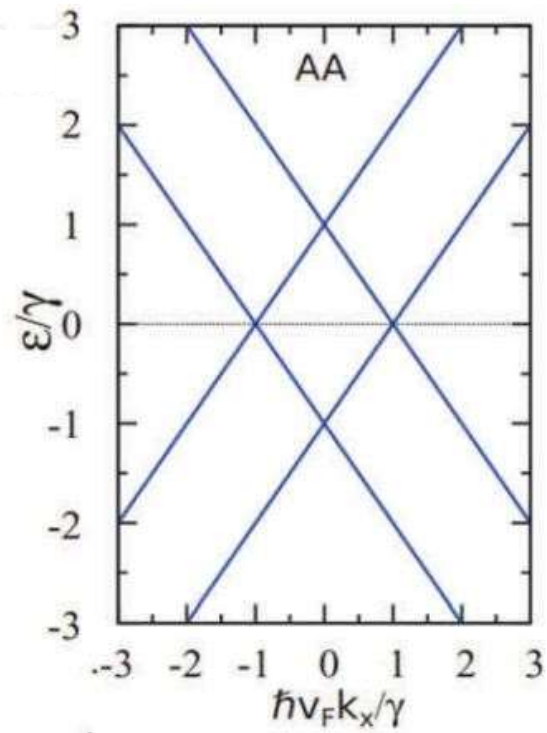
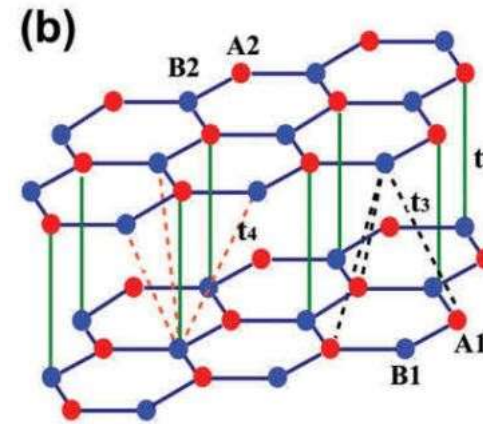
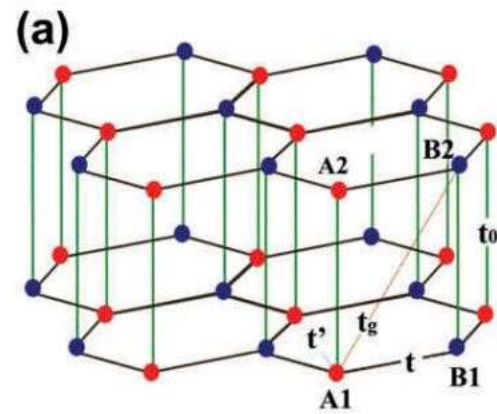


Haldane, Nobel lecture

Kane-Mele model

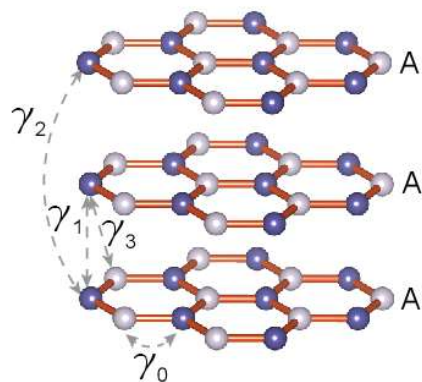


Bilayer graphene

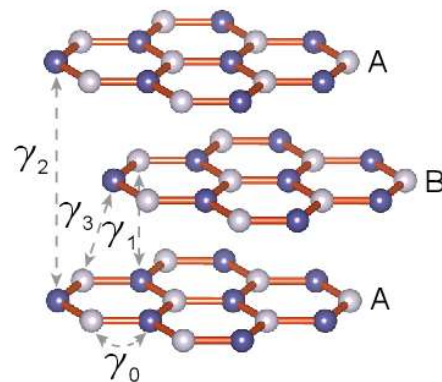


Trilayer graphene

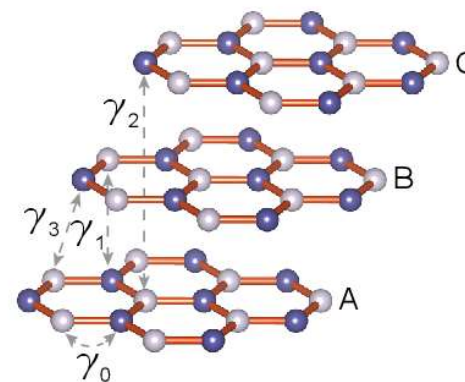
(a) simple hexagonal (AAA)



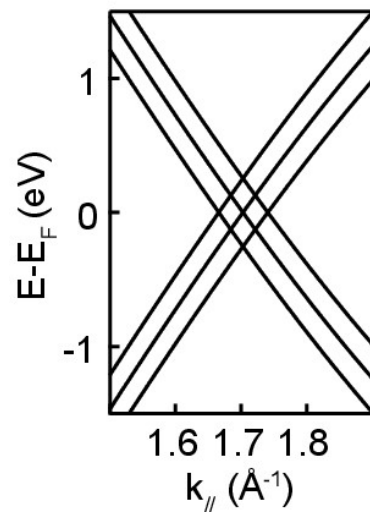
(b) Bernal (ABA)



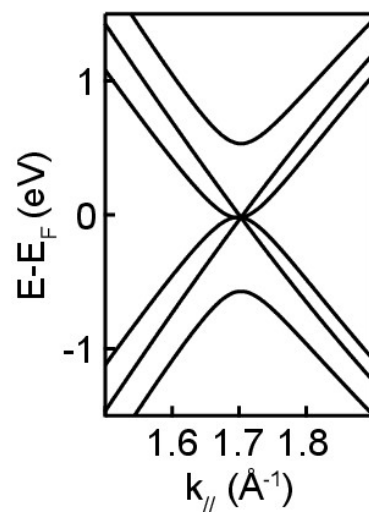
(c) rhombohedral (ABC)



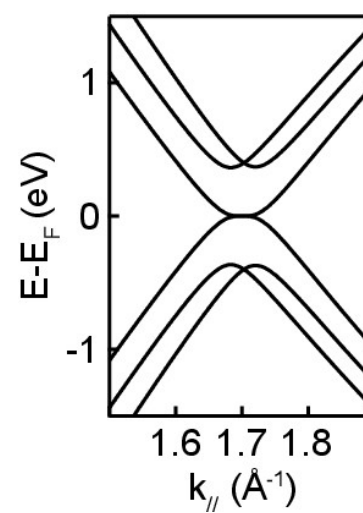
(d)



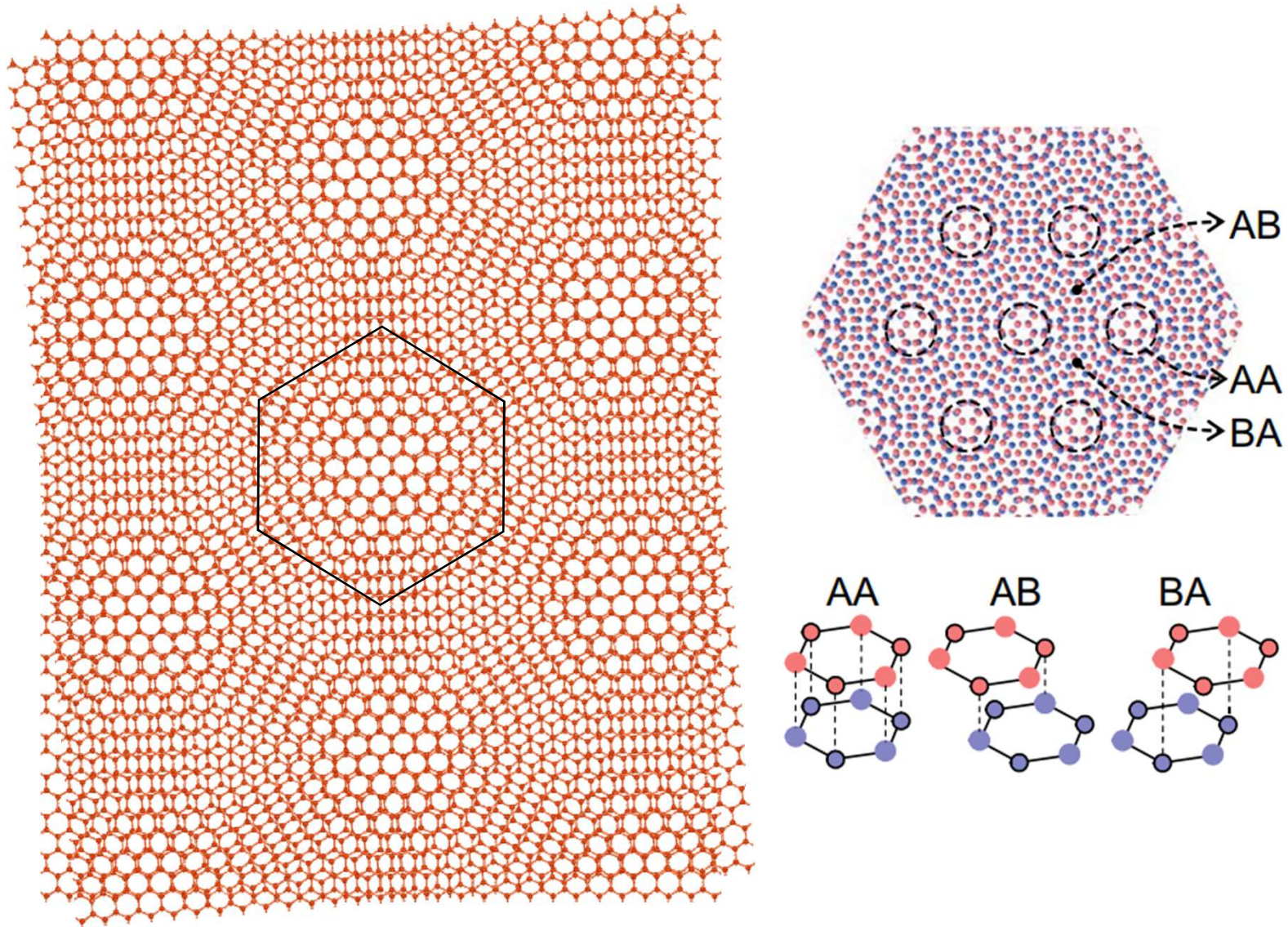
(e)

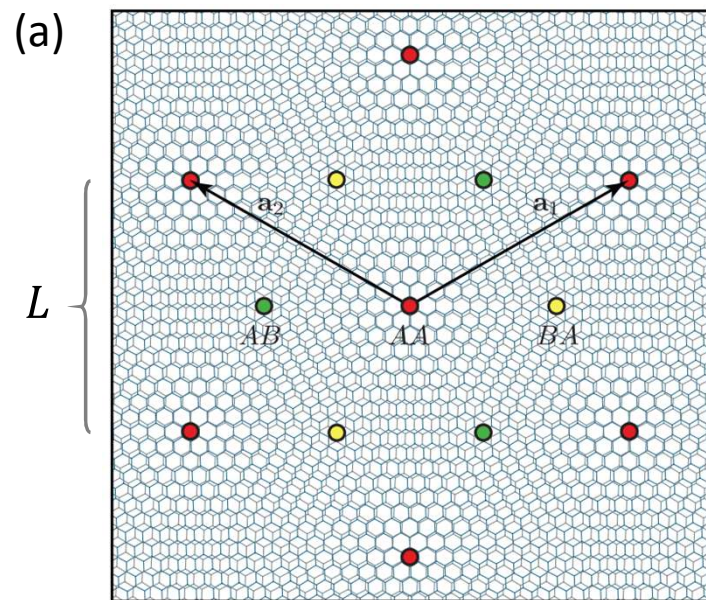


(f)

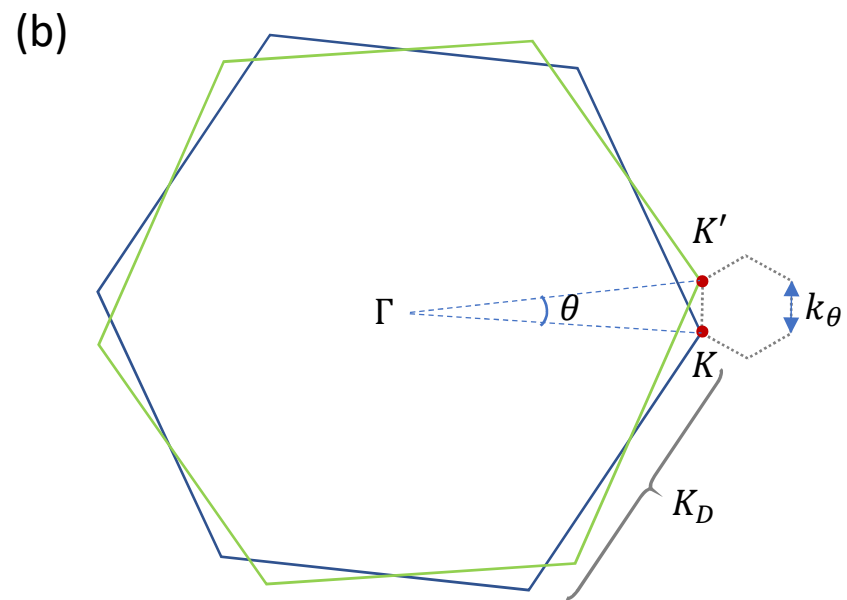


4 Twisted bi-layer graphene (TBLG) Santos et al, PRL 2007

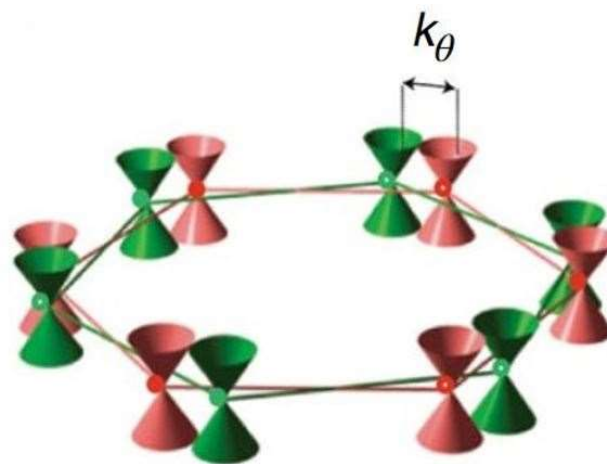




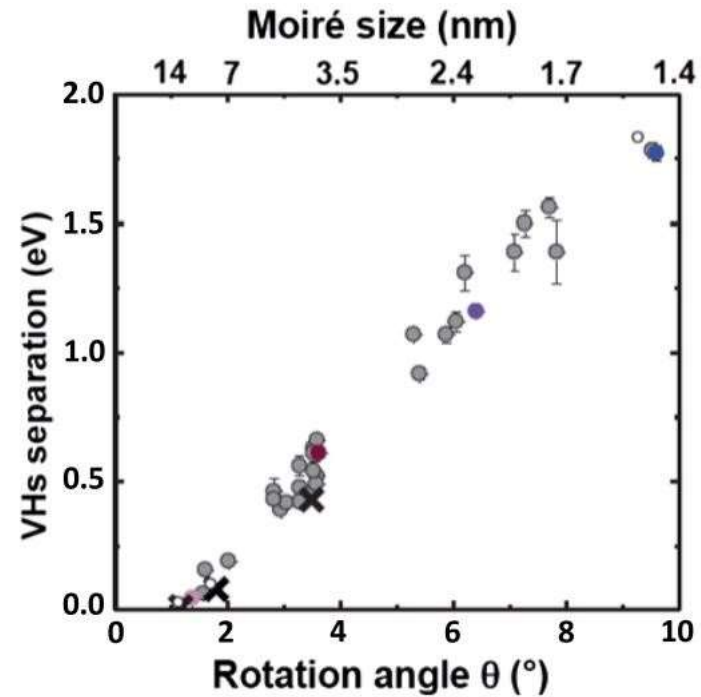
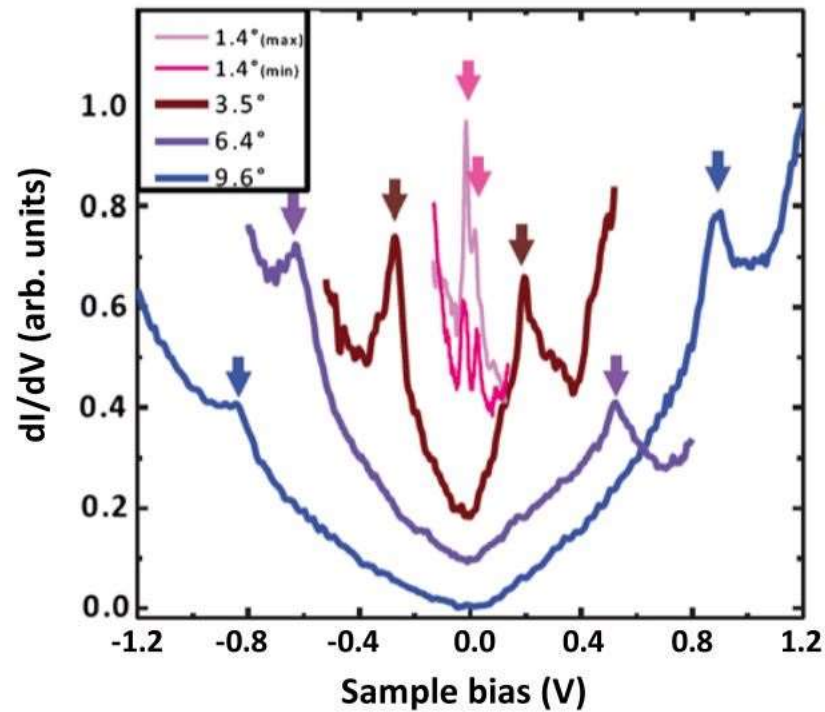
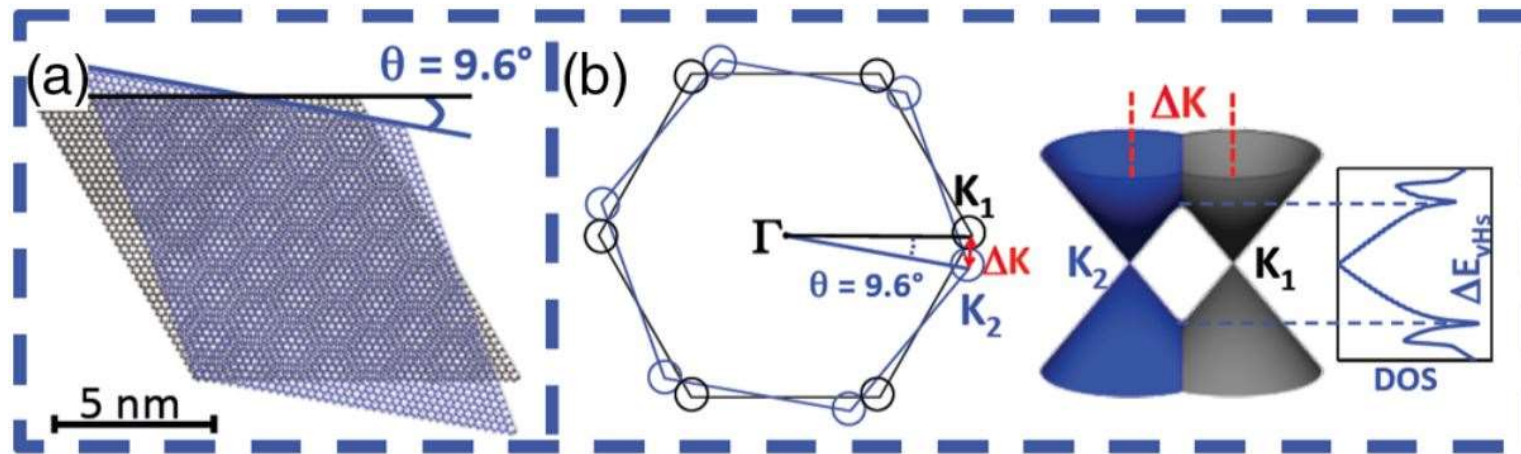
$$L = \frac{a}{2 \sin \frac{\theta}{2}}$$



$$k_\theta = 2K_D \sin \frac{\theta}{2}$$



Van Hove singularity (Li et al, Nat Phys 2010)



Predicted magic angle for flat band (Bistritzer and MacDonald PNAS 2011)

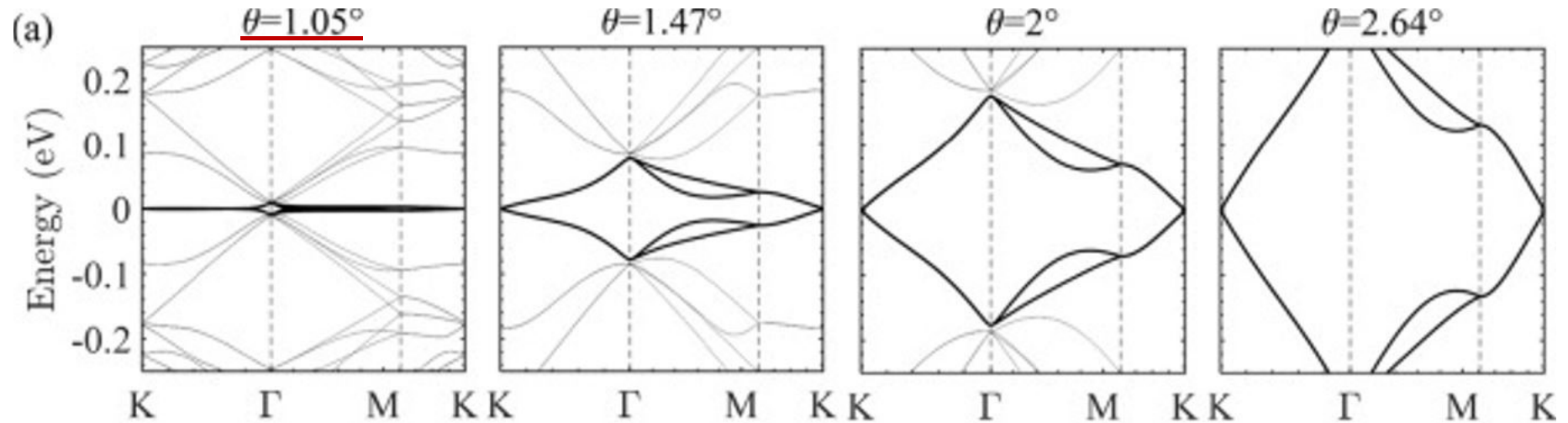
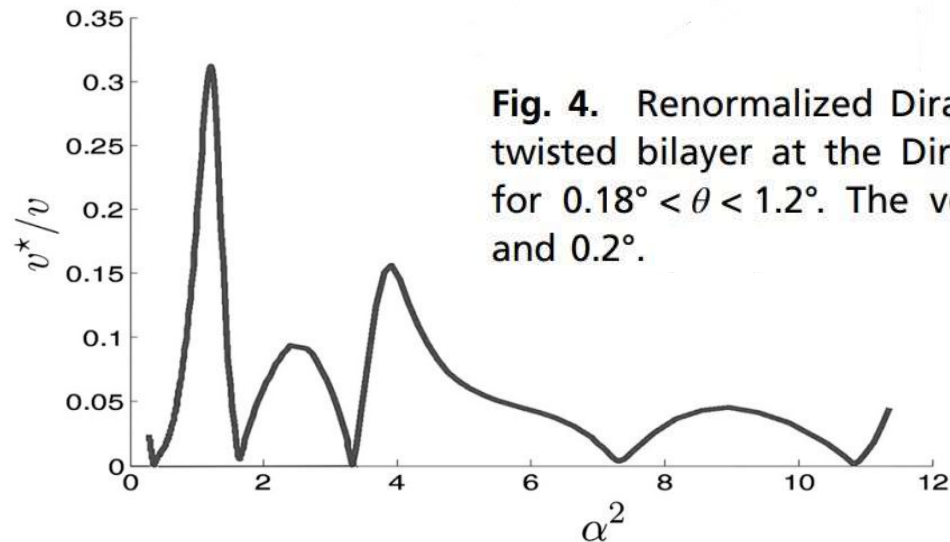
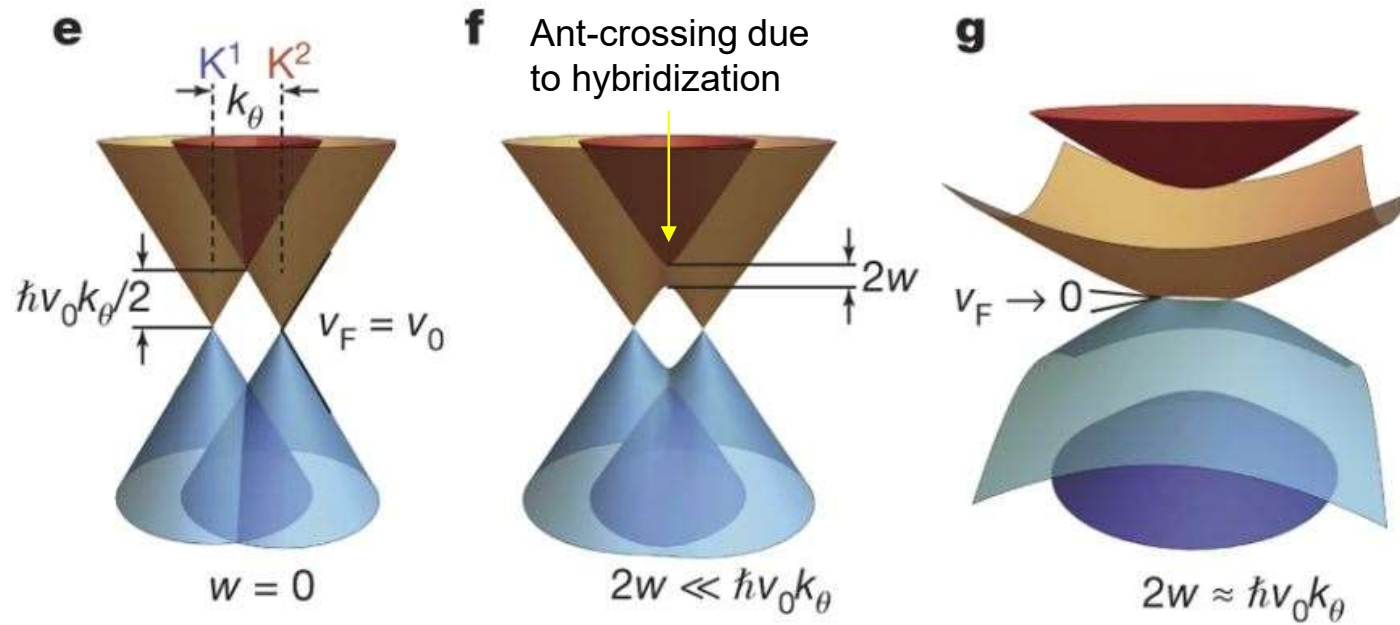


Fig from Xiong et al, Phys Lett A 2023



Flat band condition



$$\hbar v_F \frac{k_\theta}{2} = w \simeq 0.1 \text{ eV}$$

$$\hbar v_F = \frac{3}{2} a t_1$$

$$k_\theta = 2K \sin \frac{\theta}{2}$$

$$K = \frac{4\pi}{3\sqrt{3}a}$$

$$\Rightarrow \theta = \frac{\sqrt{3}w}{\pi t_1} \simeq 1.17^\circ$$

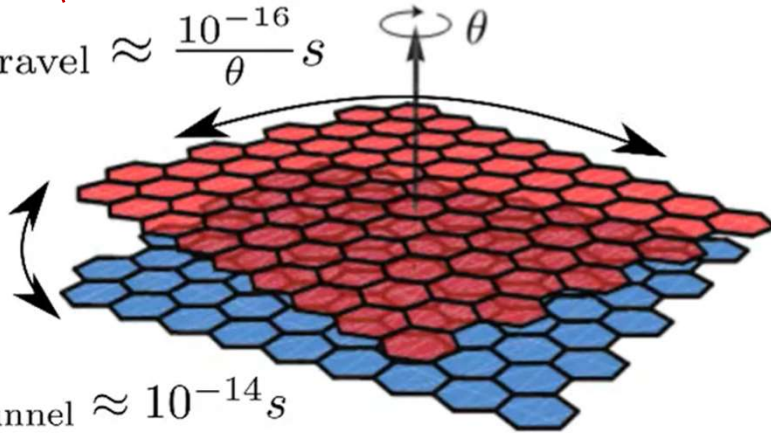
Why are we interested in flat (narrow) bands?

- Flat band dispersion \rightarrow small kinetic energy \rightarrow enhanced correlations



$$E = \cancel{K} + U$$

$$t_{\text{travel}} \approx \frac{10^{-16}}{\theta} \text{ s}$$



$$t_{\text{tunnel}} \approx 10^{-14} \text{ s}$$

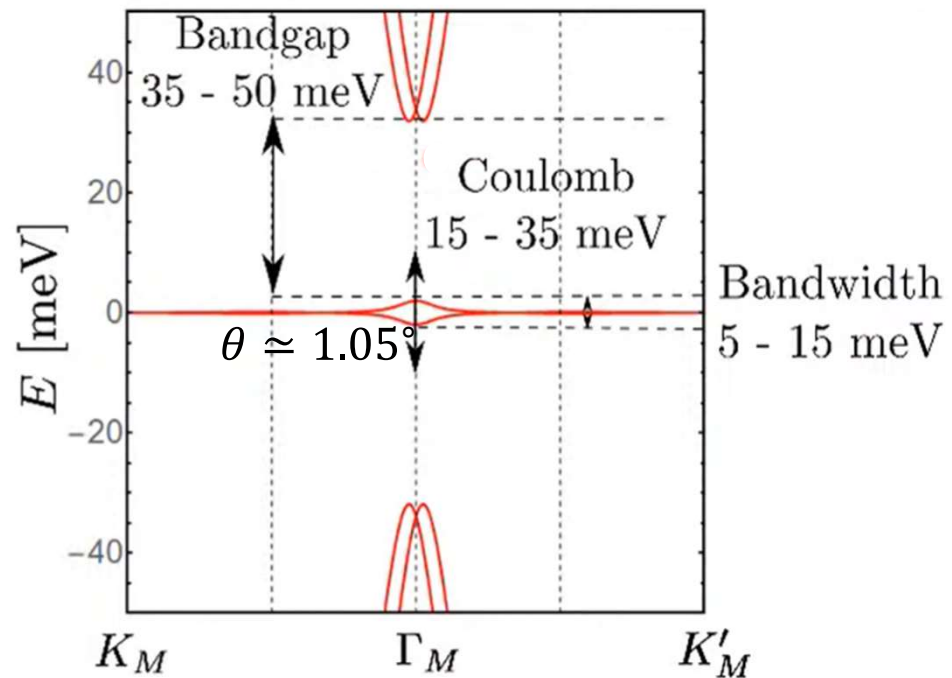
- Mott insulator
- CDW (nematic order)
- Superconductivity
- Chern insulator
- Fractional Chern insulator
- Ferromagnetism
- ...

Systems with flat bands

- Landau levels (Quantum Hall systems), need B field.
- Twisted bilayer (trilayer...) graphene
- Twisted bilayer TMD or other superstructures
- Heavy fermion materials
- ...

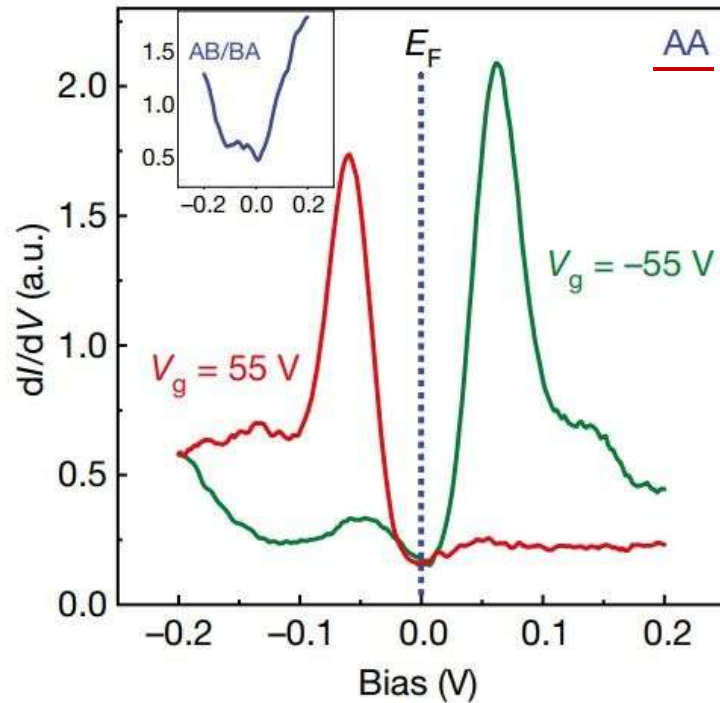
[Magic-Angle Graphene Superlattices](#): Pablo Jarillo-Herrero

Energy scales in Magic Angle TBG

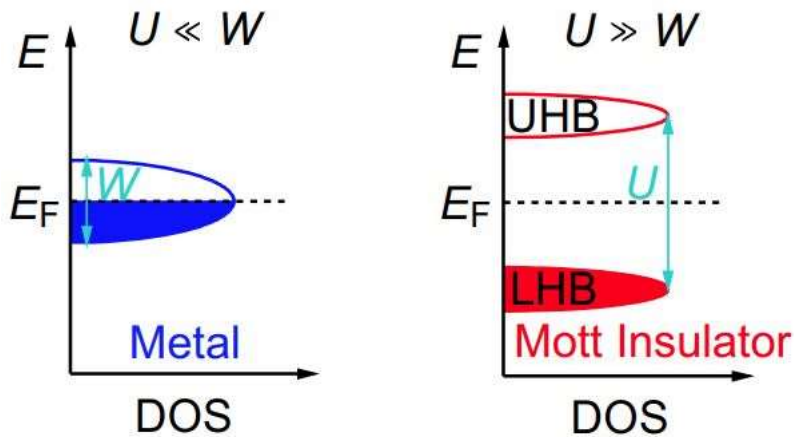
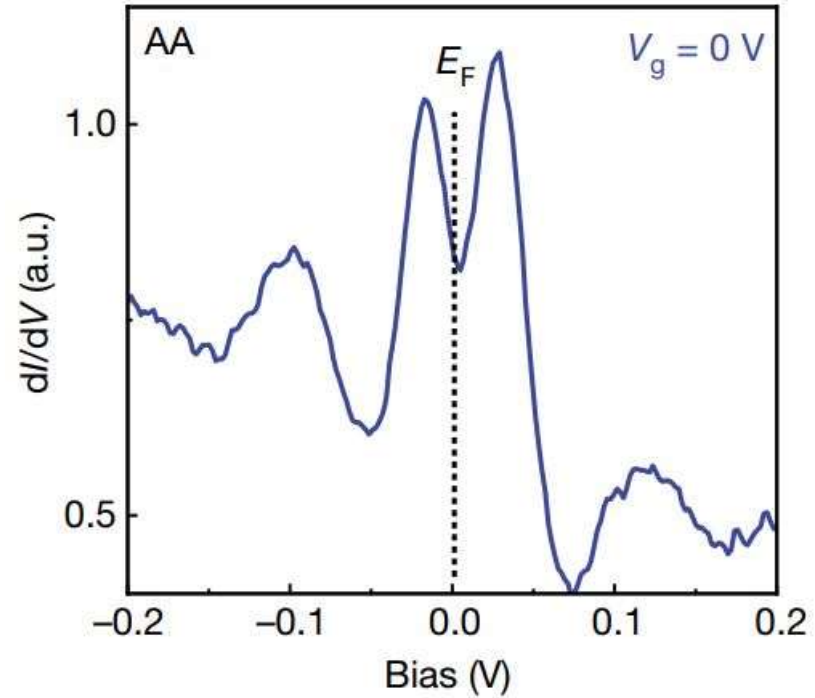


- Without spin, there are 2+2 nearly flat electron+hole bands.
- With spin, there are 4+4 bands, and the range of filling factor $\nu = [-4, 4]$ (ν = number of carriers/moire cell)

Red: fully occupied Green: fully empty
(under flat-band condition)



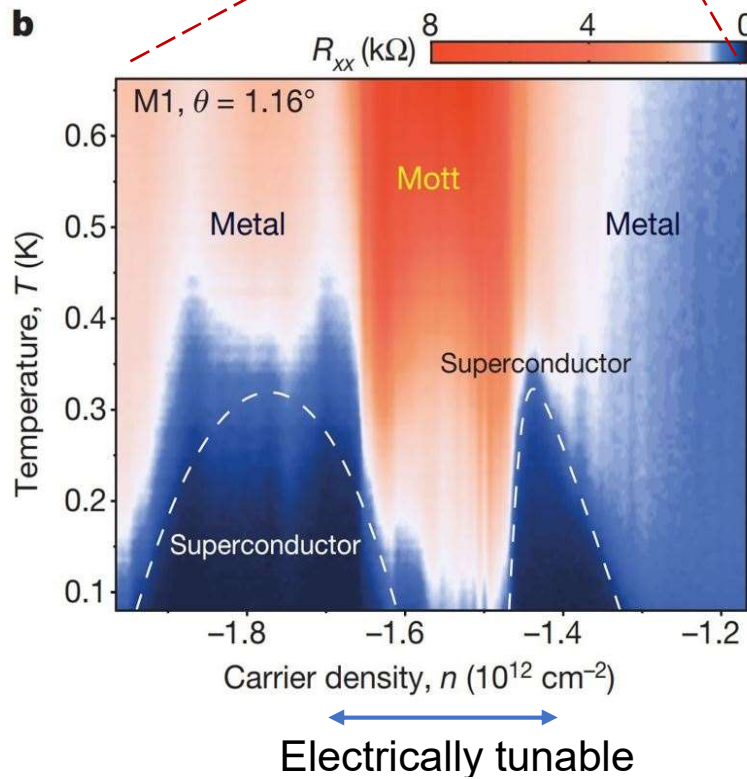
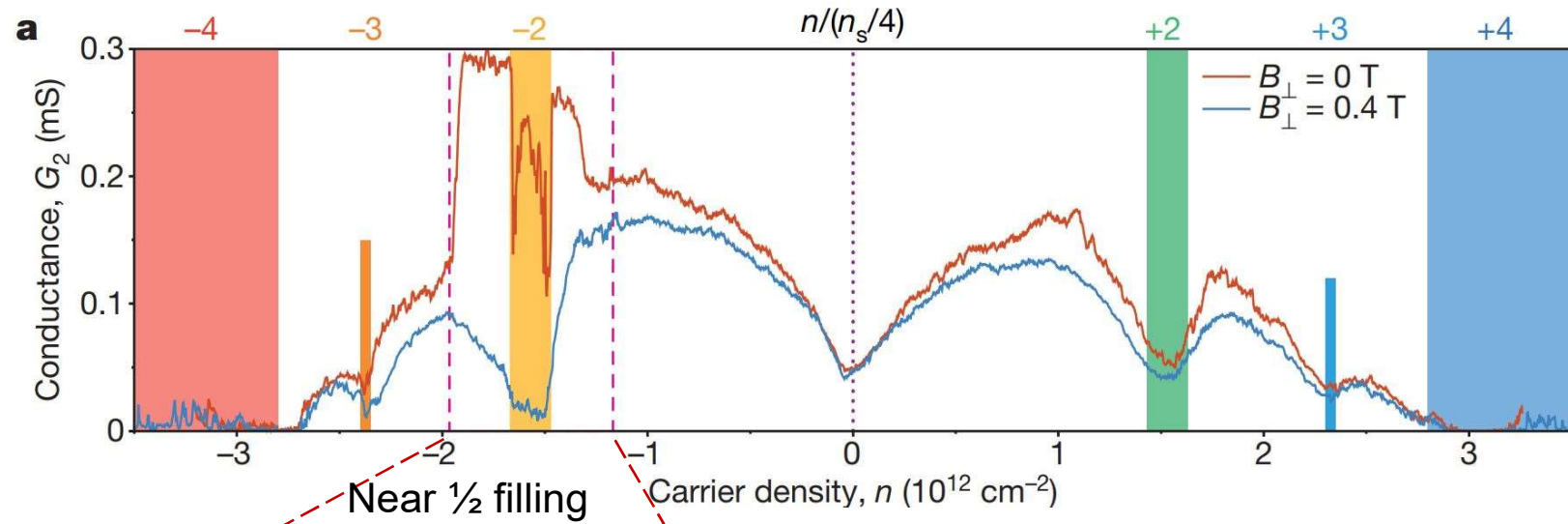
Near half-filled regime



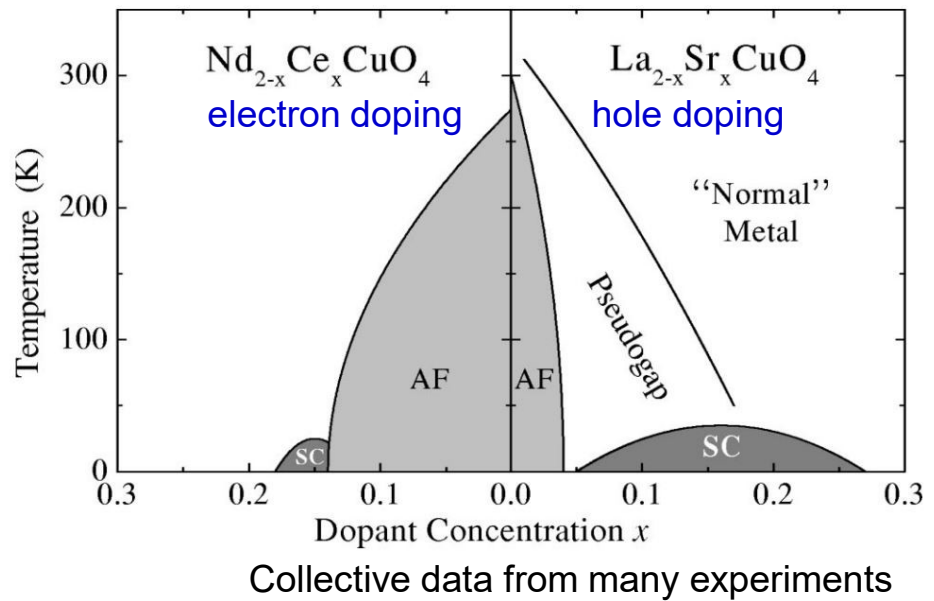
Interaction-induced energy gap
(~ Mott insulator)

Superconductivity in TBG ($T_c \sim 1.7$ K)

Cao et al, Nature 2018



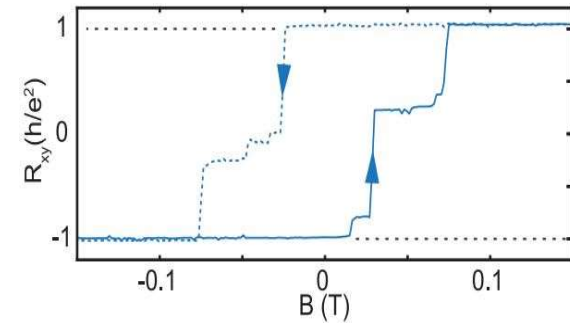
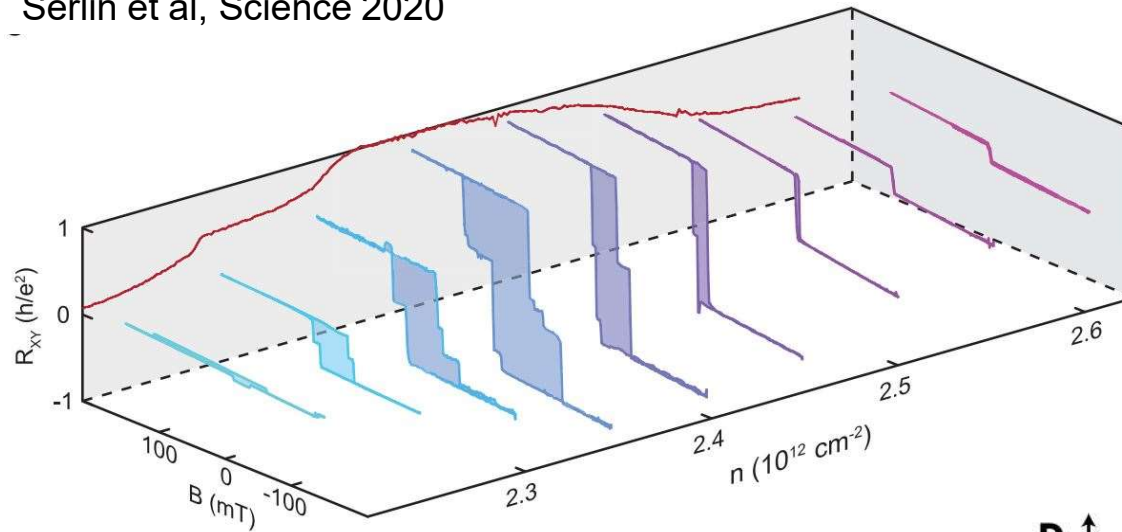
High- T_c superconductivity



Damascelli et al, RMP 2003

Quantized anomalous Hall effect in twisted bilayer graphene at 1.6 K

Serlin et al, Science 2020



Schematic band structure at full filling of a moiré unit cell ($\nu = 4$) and $\nu = 3$

Spontaneous spin and valley polarization

The topology of $|C|=1$ flat band \sim that of LLs

[Topology and broken symmetry of excitons in two-dimensional materials](#), by Sid Parameswaran

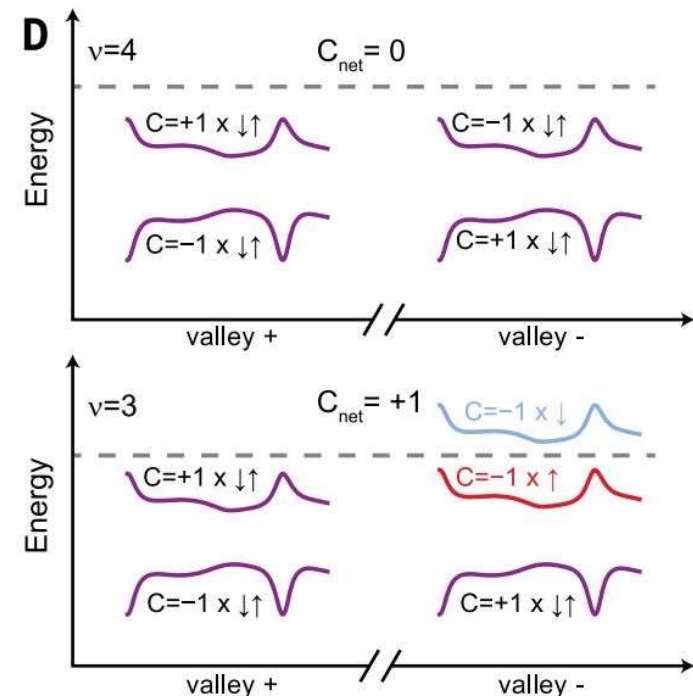
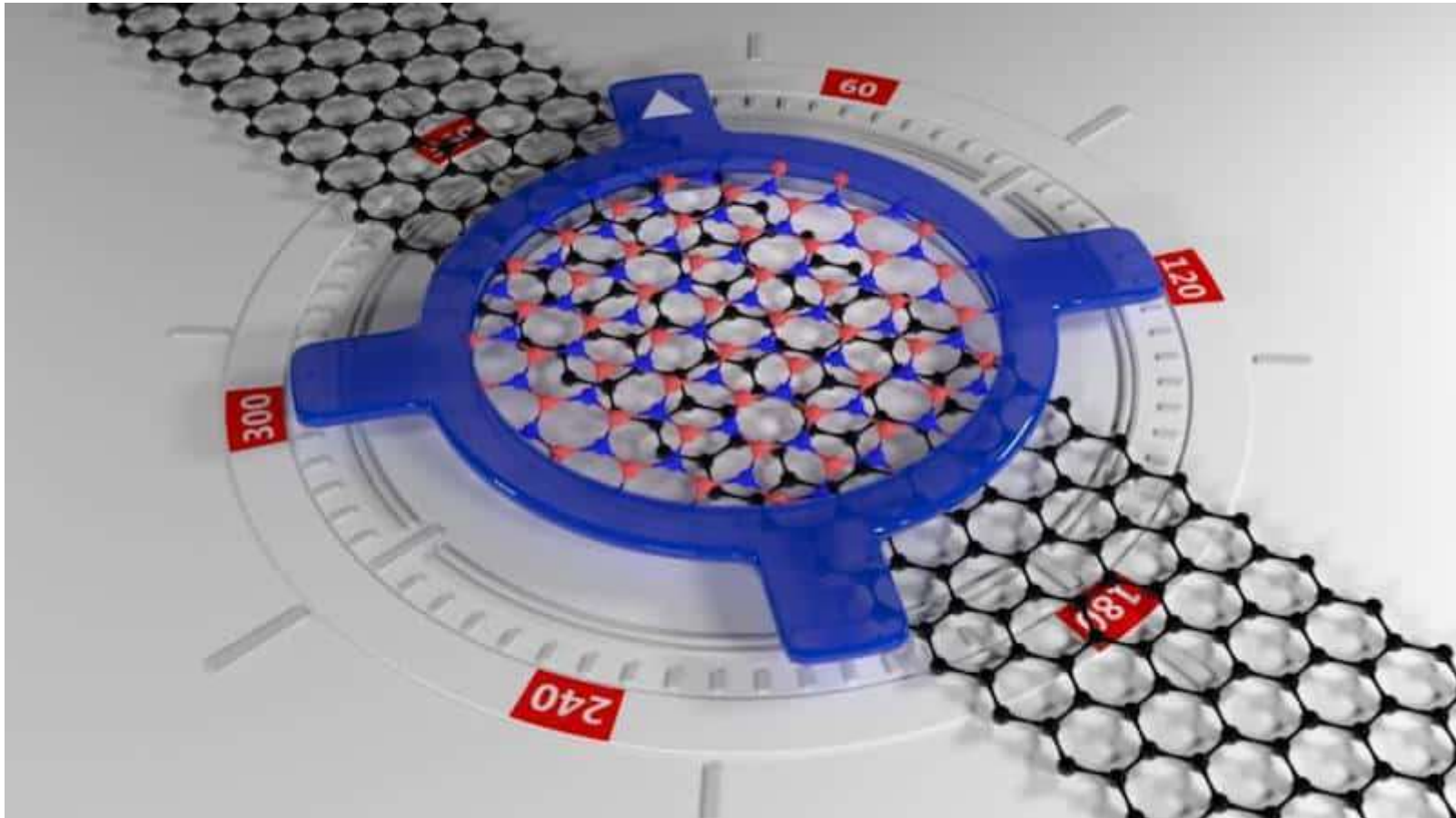


Table 1 | Advantages offered by moiré superlattices compared with atomic lattices in the exploration of Berry physics

Parameter	Atomic 2D lattices	Moiré 2D lattices
Lattice period l	$\sim 0.1 \text{ nm}$	$\sim 10 \text{ nm}$
Bandgap Δ	$\sim 1 \text{ eV}$	$\sim 10 \text{ meV}$
Berry curvature of gapped graphene $\Omega^z(k) = \frac{(\hbar v_F)^2 \Delta}{2[(\hbar v_F k)^2 + \Delta^2]^{3/2}}$ At $k = 0$: $\frac{\Omega^z(k=0)}{(\hbar v_F)^2} = \frac{1}{2\Delta^2}$	$\sim \frac{1}{1 \text{ eV}^2}$	$\sim \frac{1}{0.01 \text{ eV}^2}$
Berry curvature $[r_i, r_j] = i\epsilon^{ijk}\Omega(k) \Rightarrow \Omega(k) \sim l^2$	$\sim (0.1 \text{ nm})^2$	$\sim (10 \text{ nm})^2$
Berry curvature dipole $\text{BCD } \hbar \propto \int f(E) \frac{\partial \Omega(k)}{\partial k} dk$ BCD in 2D $\sim 1/k \sim l$	$\sim 0.1 \text{ nm}$	$\sim 10 \text{ nm}$
<u>Tunable gap</u>	Some, such as bilayer graphene	Yes, mostly
<u>Tunable Fermi velocity</u>	No	Yes
<u>Tunable Berry curvature dipole</u>	Yes, in WTe_2	Yes, with electric field and density of carriers
<u>Tunable valley Chern transitions</u>	No	Yes

Highly tunable: Twist angle, gate bias, strain ... etc

➔ **Twistronics** (Carr PRB 2017)

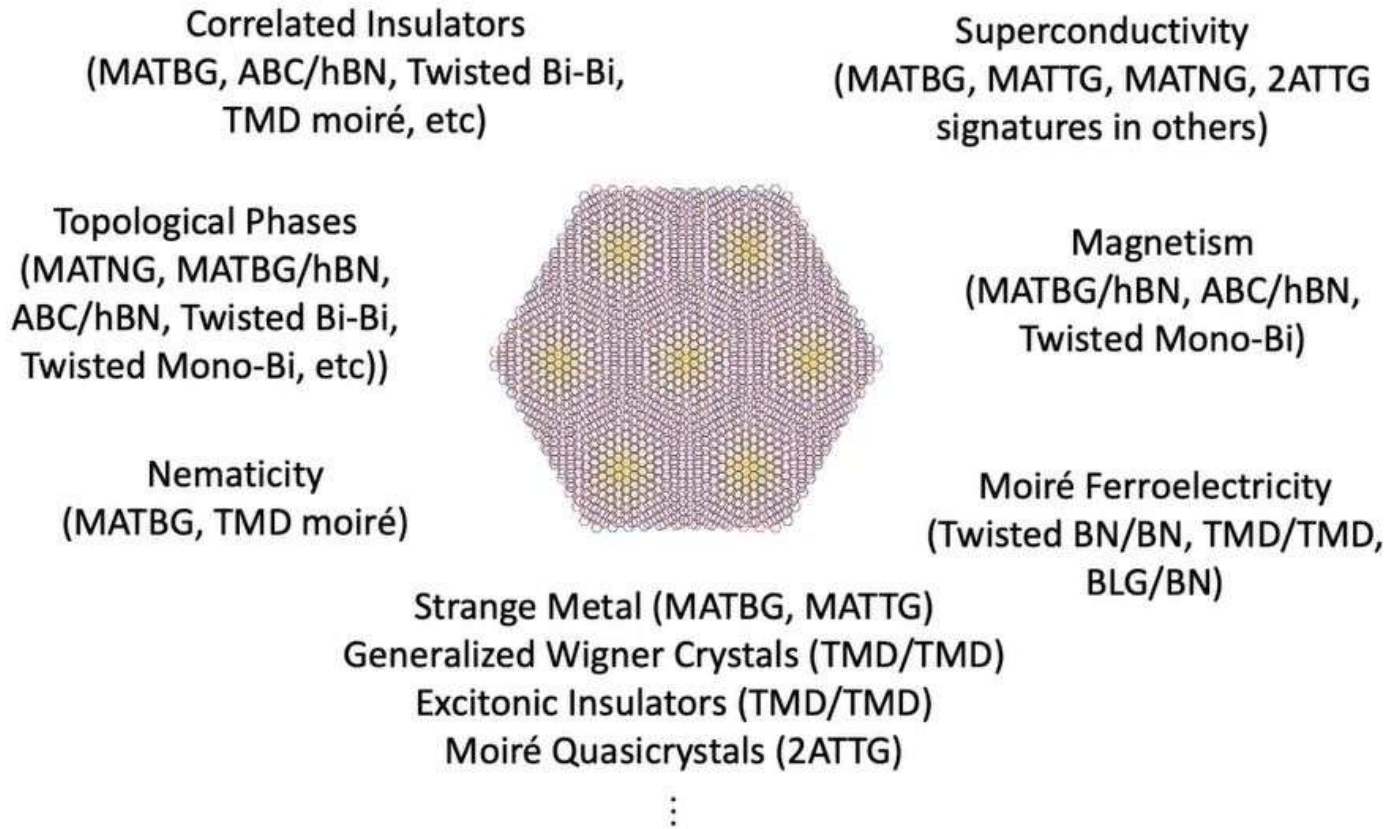


See [Twistronics@wikipedia](https://en.wikipedia.org/wiki/Twistronics)

Twisted bilayer graphene

- [Integer quantum Hall effect](#) (Lee et al, Phys Rev Lett 2011)
- [Hofstadter butterfly](#) (Hunt et al, Science 2013)
- Fractal quantum Hall effect (Dean et al, Nature 2013)
- [Fractional quantum Hall effect](#) (Wang et al, Science 2015)
- [Insulating state](#) at half filling (Cao et al, Nature 2018)
- [Superconducting states](#) (Cao et al, Nature 2018)
- Orbital ferromagnetism (Sharpe et al, Science 2019)
- [Quantum AHE](#) (Serlin et al, Science 2019)
- [Chern insulators](#) (Nuckolls et al, Nature 2020)
- [Fractional Chern insulator](#) (Xie et al, Nature 2021)
- BCD, nonlinear Hall effect (Sinha et al, 2204.02848)
- ...

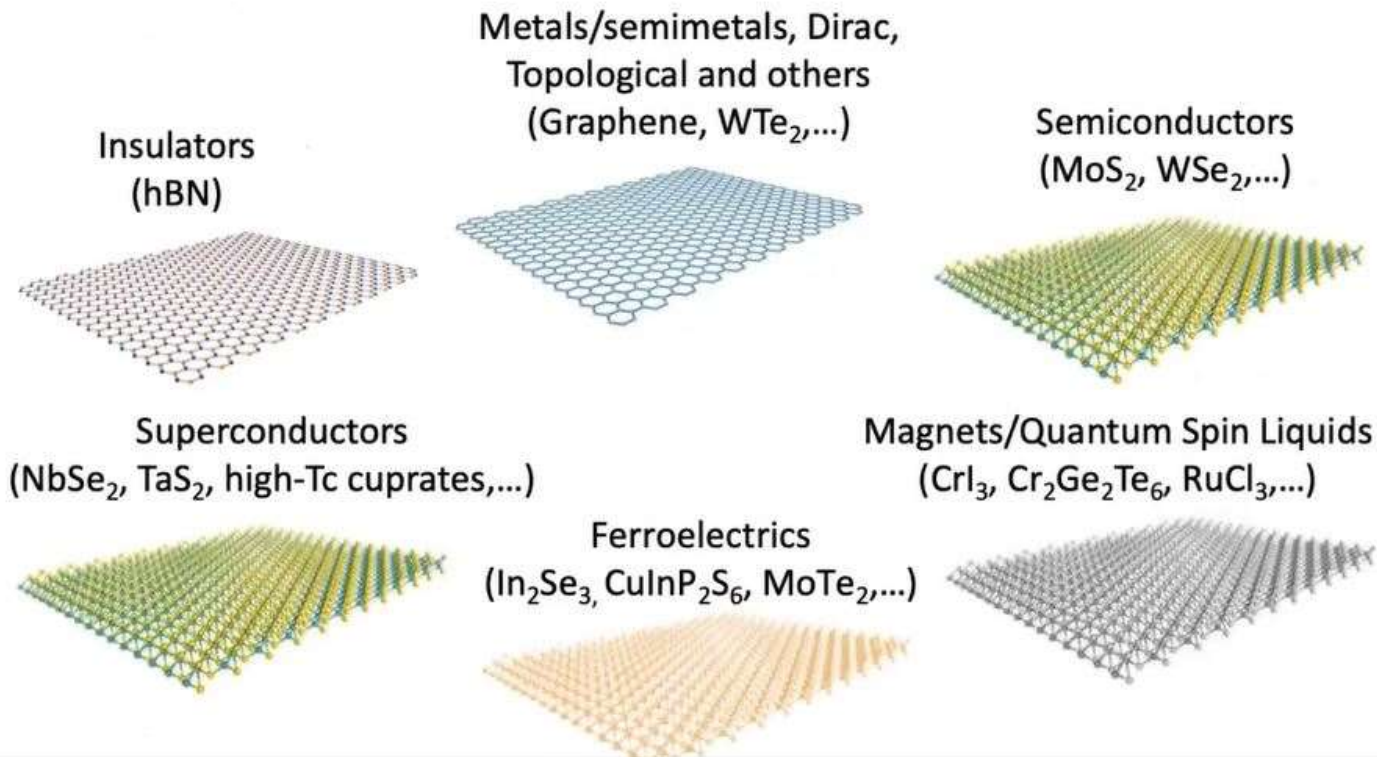
A platform for rich physics



From Pablo Jarillo-Herrero's talk @ Aspen 2023

Beyond graphene layers

With hundreds of 2D van der Waals materials... we have barely started to scratch the surface of the moiré quantum matter universe...



From Pablo Jarillo-Herrero's talk @ Aspen 2023